International Journal of Vaccine Theory, Practice, and Research

IJVTPR

Dark -Field Microscopic Analysis on the Blood of 1,006 Symptomatic Persons After Anti-COVID mRNA Injections from Pfizer/BioNtech or Moderna

Riccardo Benzi Cipelli, MD, DDS[1], Franco Giovannini, MD[2], and Gianpaolo Pisano, MD, OHNS[3]

[1] Surgeon, Specialist in Odontostomatology, Periodontologist, Studio Benzi Dental Clinic, Vigevano (corresponding author Via P. Mascagni, 41, 27029 Vigevano – Pavia, Mantua, Italy, r.riccardo.benzi.cipelli@gmail.com)

[2] Surgeon, Acupuncture Specialist, Oxygen-Ozone therapy, Diagnostics, Giovannini Biodiagnostic Center, AMBB Headquarters, Mantua, Italy

[3] Surgeon, Specialist in Otolaryngology, Masters in Cytology

ABSTRACT

The use of dark-field microscopic analysis of fresh peripheral blood on a slide was once widespread in medicine, allowing a first and immediate assessment of the state of health of the corpuscular components of the blood. In the present study we analyzed with a dark-field optical microscope the peripheral blood drop from 1,006 symptomatic subjects after inoculation with an mRNA injection (Pfizer/BioNTech or Moderna), starting from March 2021. There were 948 subjects (94% of the total sample) whose blood showed aggregation of erythrocytes and the presence of particles of various shapes and sizes of unclear origin one month after the mRNA inoculation. In 12 subjects, blood was examined with the same method before vaccination, showing a perfectly normal hematological distribution. The alterations found after the inoculation of the mRNA injections further reinforce the suspicion that the modifications were due to the so-called "vaccines" themselves. We report 4 clinical cases, chosen as representative of the entire case series. Further studies are needed to define the exact nature of the particles found in the blood and to identify possible solutions to the problems they are evidently causing.

Keywords: *blood from COVID-19 vaccine recipients, dark-field microscopy, detoxification of COVID-19 inoculation recipients, experimental injections, foreign materials in COVID-19 injections*

Introduction

Dark-field microscopic analysis of fresh blood on a slide was once widely used in medicine. It enabled an immediate assessment of the state of health of the corpuscular components of the blood. The traditional analysis would proceed to completion with measurement of acidity versus alkalinity (pH), relative hydrogen (rH2), and rate of oxygen release (rO2). These measures (not shown in this paper) would help to define early on any harmful blood alterations even before they could be revealed by coagulation measures of D-dimer (DD), prothrombin time (PT), partial thromboplastin time (PTT), fibrinogen (Fg), platelet counts, and so forth (Long et al., 2020; Giovannini & Pisano, in press). The present study presents the results of

dark-field microscopic analysis of the blood of 1,006 patients referred to the "Giovannini Biodiagnostic Center" for various disorders after inoculation with mRNA injections (Pfizer/BioNTech or Moderna). Of the total 1,006 subjects, blood drops from 12 of them were performed, prior to any mRNA injections, using the same dark-field microscopic methods. Of these 12 subjects, 4 were chosen as representative of the entire sample of 1,006 cases and are reported in detail as illustrated with corresponding photographic images.

MATERIALS AND METHODS

With a dark-field optical microscope, we analyzed peripheral blood, a drop of it from each of 1,006 symptomatic subjects after at least one mRNA injection (Pfizer or Moderna), starting from March 2021. All the demographic data and the basic statistics are summarized in Table 1.

Table 1
Demographic Data on Cases Studied with Dark-Field Microscopy

Grouping by Age	Males	%	Females	%	All	%
10-20	16	3.76%	4	0.69%	20	1.99%
21-30	29	6.81%	25	4.31%	54	5.37%
31-40	105	24.65%	43	7.41%	148	14.71%
41-50	102	23.94%	120	20.69%	222	22.07%
51-60	138	32.39%	255	43.97%	393	39.07%
61-70	29	6.81%	114	19.66%	143	14.21%
71-80	7	1.64%	14	2.41%	21	2.09%
81-90	0	0.00%	5	0.86%	5	0.50%
Column Totals (Check Sum)	426	100.00%	580	100.00%	1,006	100.00%

Doses Received	Males	%	Females	%	All	%
1 dose	72	16.90%	69	11.90%	141	14.02%
2 doses	168	39.44%	285	49.14%	453	45.03%
3 doses	186	43.66%	226	38.97%	412	40.95%
Column Totals (Check Sum)	426	100.00%	580	100.00%	1,006	100.00%

	Males	%	Females	%	All	%
Cases with Normal Blood	27	2.68%	31	3.08%	58	5.77%
Cases with Abnormal Blood	399	97.32%	549	96.92%	948	94.23%

Of the 1,006 subjects, 426 were males and 580 were females and 141 of them received only a single dose of the mRNA experimental injection, 453 got a second dose, and 412 received a third dose. The average age of the 1,006 subjects was 49 years and their age ranged from 15-85. On the average, 5.77% of the 1,006 individuals had normal blood samples in spite of their COVID-19 symptoms. The remaining 94.23% had abnormal blood samples as illustrated in the 4 cases we selected out of the 12 who were normal before receiving any mRNA injections but were no longer normal afterward. For each case, a drop of blood was drawn by pricking a finger and was analyzed under a ZEISS Primostar or LEITZ Laborlux 12 dark-field microscope. The observation of the blood under an optical microscope in a dark-field took place an average of thirty days after the last inoculation. From a minimum of 5 to a maximum of 20 photographs were taken for each patient examined. All initial observations were made at 40x magnification except for digital 3x enlargements to 120x for certain objects of interest. Measurements were performed with DeltaPix InSight Software.

RESULTS

Of the 1,006 cases analyzed, only 58 (27 males and 31 females), equal to 5.77% of the total, presented a completely normal hematological picture upon microscopic analysis after the last mRNA injection with either the Moderna or Pfizer concoction. The vaccines are purported to contain at least the spike protein from SARS-CoV-2 (Nance & Meier, 2021), but is known also to contain foreign particles that the CDC and the many promoters of the experimental injections claimed were not in them at all. Among those foreign components are metallic objects as demonstrated previously in this journal by Lee et al. (2022) which are confirmed in our results as described in the following. The 4 clinical cases reported below, with photographic documentation revealing strange phenomena in their blood, illustrate the range and types of the anomalies found in the microscopic examination of the blood of 94.23% of the 1,006 cases (a total of

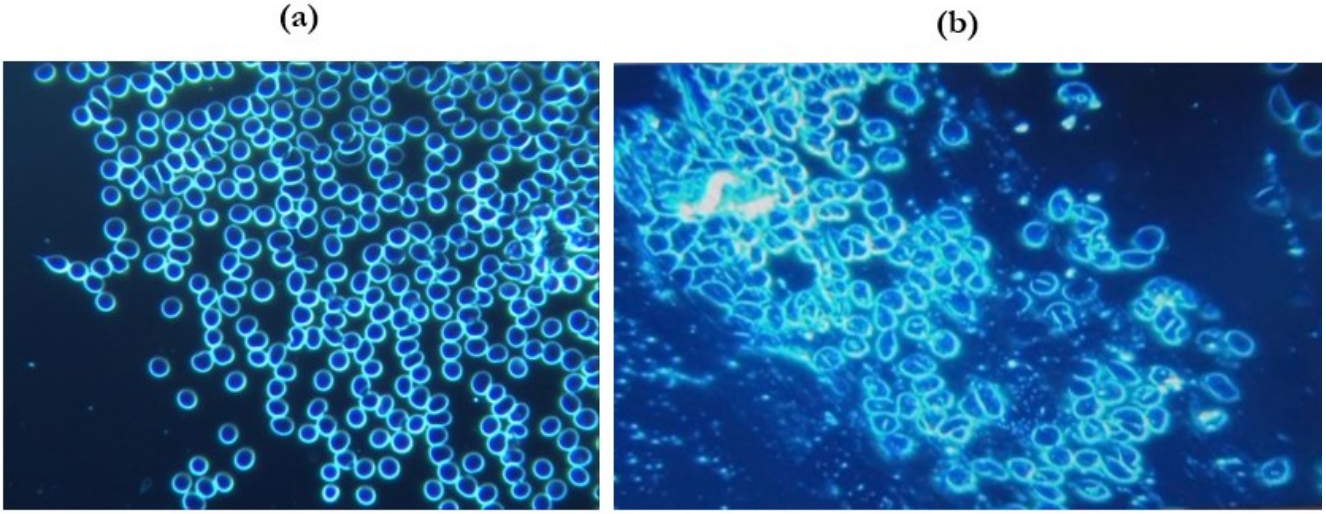

Figure 1. These photos are at 40x magnification. At the left side, (a) shows the blood condition of the patient before the inoculation. The right side image, (b) shows the same person's blood one month after the first dose of Pfizer mRNA "vaccine". Particles can be seen among the red blood cells which are strongly conglobated around the exogenous particles; the agglomeration is believed to reflect a reduction in zeta potential adversely affecting the normal colloidal distribution of erythrocytes as see at the left. The red blood cells at the right (b) are no longer spherical and are clumping as in coagulation and clotting.

948 cases that showed the same sorts of abnormalities). The 4 cases summarized and illustrated here are, according to our understanding and in our opinion as clinical experts, absolutely representative of all 948 cases with peripheral blood alterations.

Figure 2. In this case the assembly of particles takes on crystalline features; furthermore, there is an area of close influence, butterfly wings, in the context of which a crystalline type organization occurs.

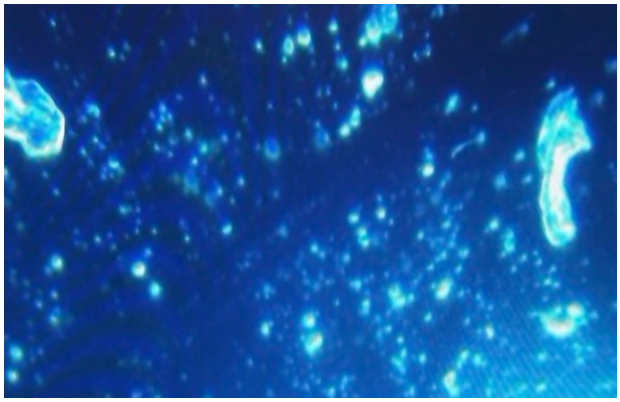

Figure 3. The image at 120x magnification shows two exogenous particles and clusters of fibrin 2 months after vaccination.

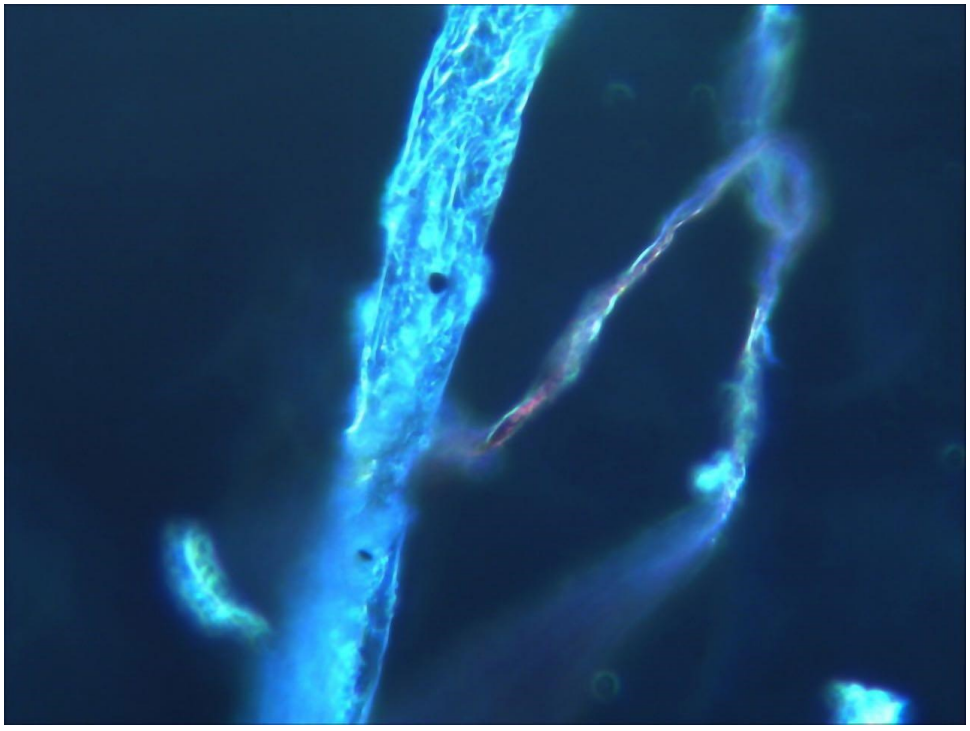

Figure 4. This image at 120x magnification (3x magnification digitally produced) highlights a typical self-aggregating structuring in fibro/tubular mode.

CASE NO. 1 (SEE FIGURES 1-6)

This individual is a male of 33 years, who formerly was an athlete, apparently healthy before inoculation with an mRNA Pfizer injection. One month after receiving the first dose of the Pfizer "vaccine", he showed marked asthenia, a constant gravitational headache (i.e., one sensitive to the position and movements of his head and body such that the pain was increased by movement of the head up or down). The headaches were unresponsive to common pain killers. Diffuse rheumatic arthralgia with dyspnea on exertion were noted.

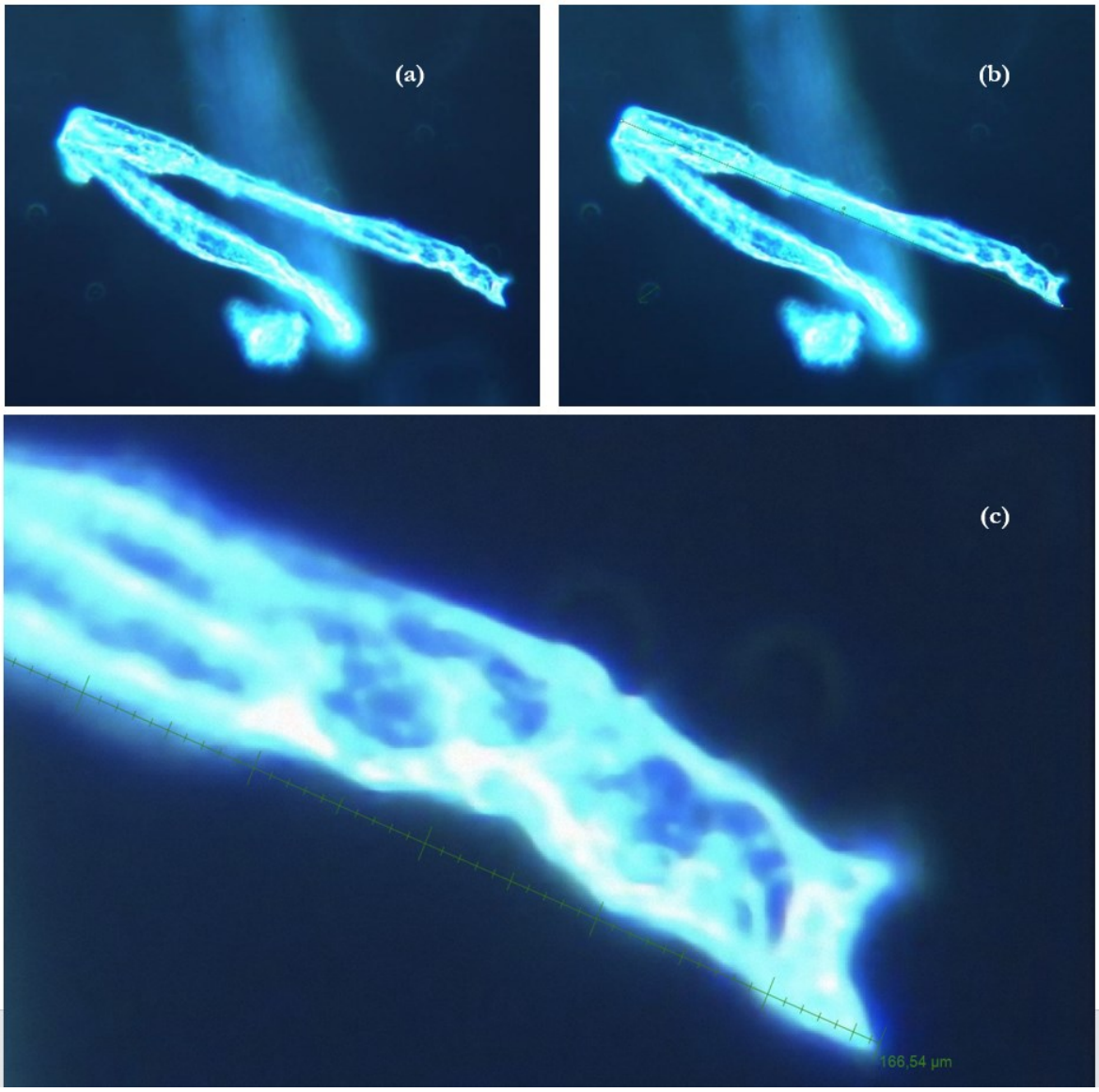

Figure 5. A highly structured fibro-tubular configuration of structures that can coalesce together, reaching dimensions ten times their initial size. In (a) and (b) at 40x magnification, we see what appears to be a laminar linkage. In (c), at 120x magnification (3x magnification digitally produced), there is a composite which is 166.54 µm (DeltaPix Software) in length.

(a) (b)

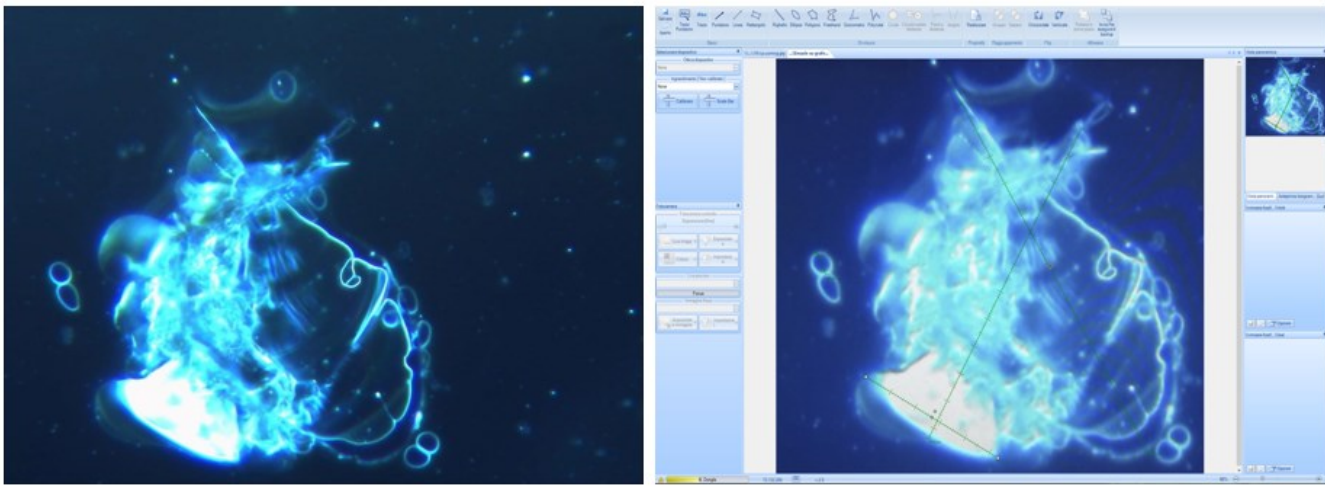

Figure 6. The sharper and larger image on the left seems to suggest the power of the exogenous particles introduced into the blood of mRNA injection recipients to assemble themselves into massive structures: we can see in both (a) and (b) at 120x magnification evidence of what appear to be lamellar configurations similar to agglomerations occurring in a field of forces pulling colloidal particles in the plasma together. The relative bulk of the particle conglobate can be easily estimated by comparison with the erythrocytes at the periphery of the much larger mass. It was also measured accurately at 113.91µm by 139.99µm (see the hatch mark green lines in b) using the Delta-Pix Software as shown in the computer screen shot at the right.

(a) (b)

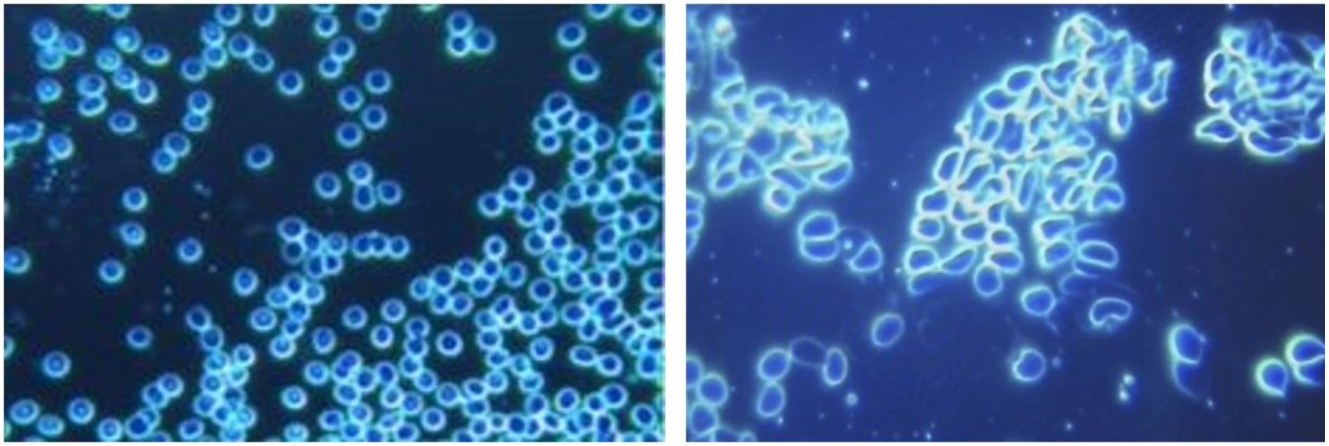

Figure 7. (a) The photo on the left at 40x magnification shows the blood condition of the patient before the inoculation. (b) The image on the right, also at 40x magnification, shows the deformation of the erythrocyte cell profile, and the strong tendency for the deformed erythrocytes to aggregate.

CASE NO. 2 (FIGURES 7-9)

This case was a woman 54 years old whose symptoms included the drug-resistant severe headache, profound worsening asthenia, sleep/wake rhythm disorders, generalized paresthesia and dysesthesia, psychic manifestations with depressive mood after the second dose of the Pfizer vaccine. Her blood story is captured in Figures 7 through 9

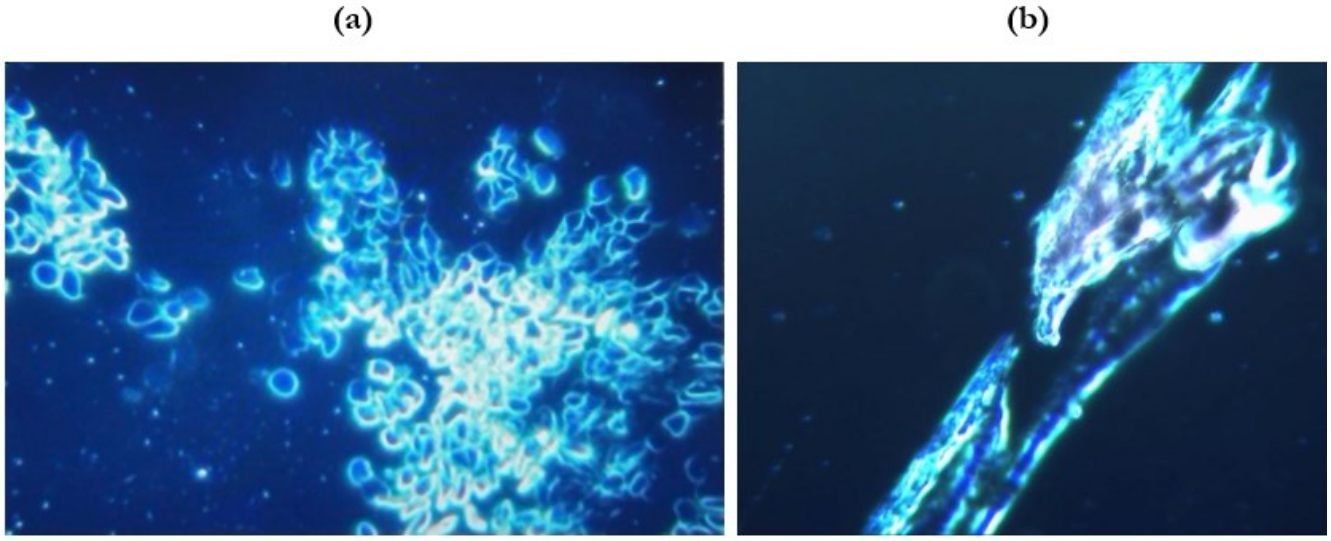

Figure 8. (a) Deformation and erythrocyte aggregation with signs of hemolysis at 40x magnification. (b) A foreign crystallized tubular structure at 120x magnification.

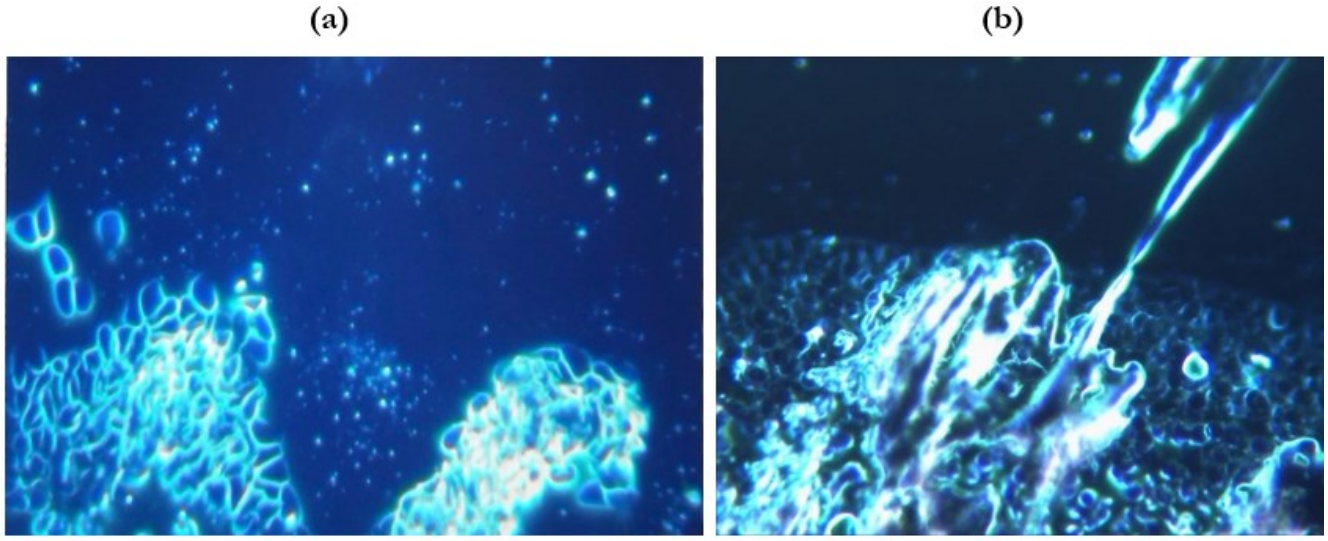

Figure 9. (a) Aggregated/conglobated erythrocytes, with hemolysis, and clustered fibrin at 40x magnification. (b) A blowup of a foreign complex crystalline structure at 120x magnification.

CASE NO. 3 (FIGURES 10-18)

This patient, in 2021, was an 84-year-old woman, enjoying managing an unassisted satisfying life with autonomy before receiving any mRNA injections. Her medications at the time included beta blocker, ace

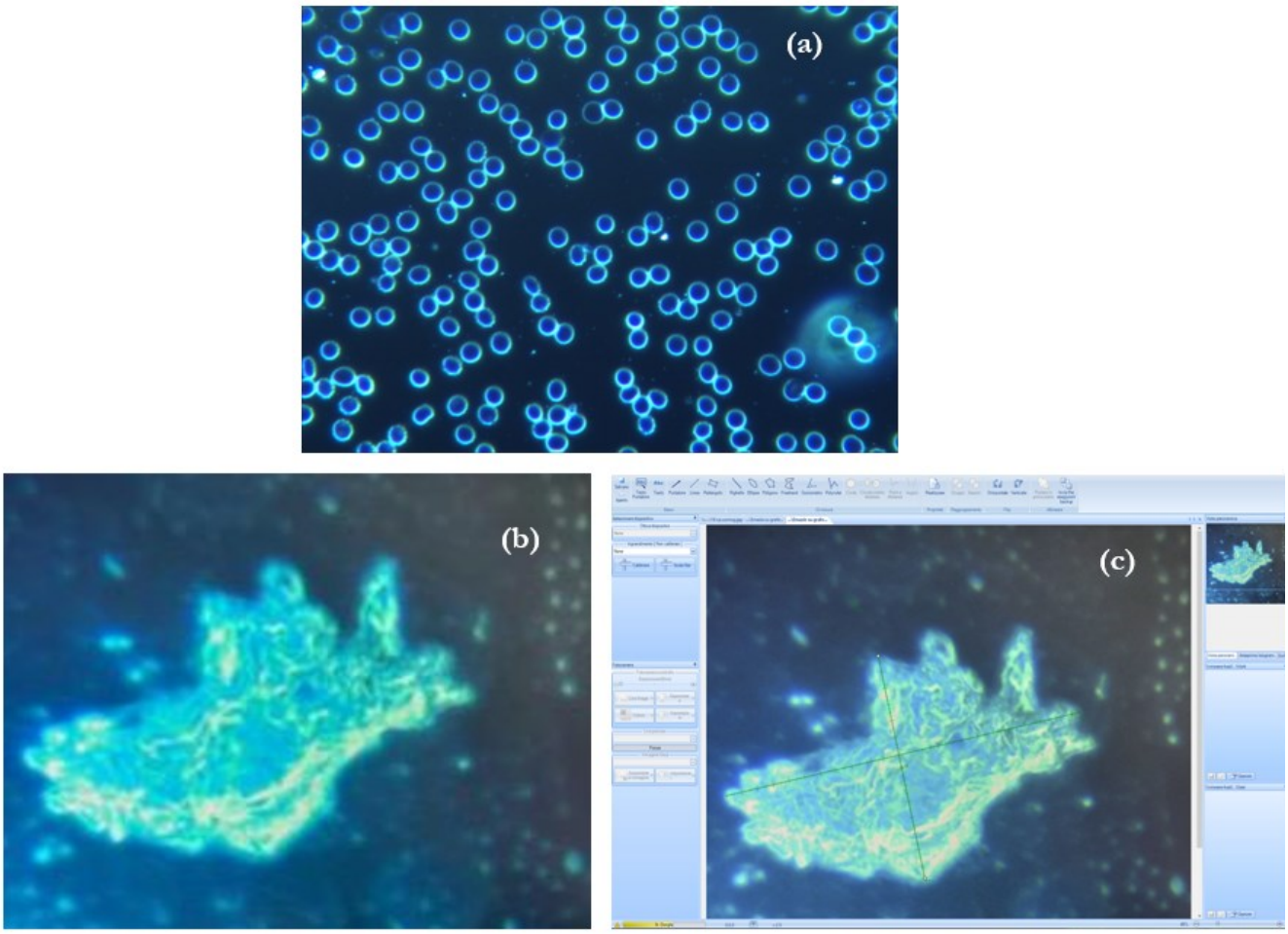

Figure 10. (a) The photo at the top and center shows the patient's blood condition at 40x magnification before the first mRNA inoculation. The images in (b) and (c), at 120x magnification, left and right at the bottom of the figure, show a voluminous agglomerate (measured at 329.14µm by 137.74µm with the DeltaPix software) five weeks after vaccination. Are these metallic objects graphene particles?

inhibitor, diuretic, cardio-aspirin, and a gastro protector. In 2016 she had been operated on for descending colon cancer without locoregional lymph nodes or metastases. She was declared free from the neoplastic pathology at the 5-year-follow-up in 2021 before receiving any mRNA injection. In 2020, she was seen for symptoms of a burning mouth that responded to topical treatment; histology was positive for a mixed lichen/pemphigus infection. She was strongly advised not to be injected with the anti-COVID-19 experimental genetic concoction. This advice was on account of her previous oncological and ongoing rheumatic disease.

In fact, at the second dose of Pfizer, she experienced intense erythroderma of the face and chest, a dramatic intensification of the burning mouth symptoms, unsustainable muscle pains resistant to analgesic therapy. Using capillaroscopy, her rheumatologist diagnosed a form of acute dermatopolymyositis which was

confirmed with self-immunity tests. The symptoms did not respond to 60 mg of deflazacort (used because she was known to be intolerant to Deltacortene, a different form of cortisone) and 10 mg per week of Methotrexate. Later, the rheumatologist suspended the Methotrexate but added 500 mg of Mycophenolate

Mofetil 3 times daily to taper down the dosage of cortisone. A tachyarrhythmia was successfully treated with TAO and Amiodarone; following a cardioversion performed in a stable electric field (3 sessions),

rivaroxaban (Xarelto), stabilized with flecainide (Almarytm). Alendronate was added (one tablet per week), cholecalciferol 50,000 IU per month, and folic acid one tablet per week. Due to abdominal pain a PET scan was carried out and ileo-aortic abdominal lymph nodes proved to be positive. A subsequent abdominal CT and MRI ruled out a neoplastic recurrence, attributing the lymphadenopathy exclusively to the worsening of the rheumatic disease which, from a mild form confined to the oral cavity, had evolved into a severe systemic form (polymyositis).

Figure 11. Geometric figures tend to take shape (120x magnification) in extremely complex aggregates.

Within a month, she was no longer autonomous. She required a walker, had developed mild renal insufficiency possibly due to an excessive pharmacological load. This escalation, which led to an authentic biological fragility, occurred chronologically later and was probably (according to our informed medical opinions) caused by the mRNA injections. Our assessment is that by injecting elderly patients who are already contending with multiple comorbidities with the experimental mRNA "vaccines", previously controlled morbidities are very suddenly augmented in a negative way.

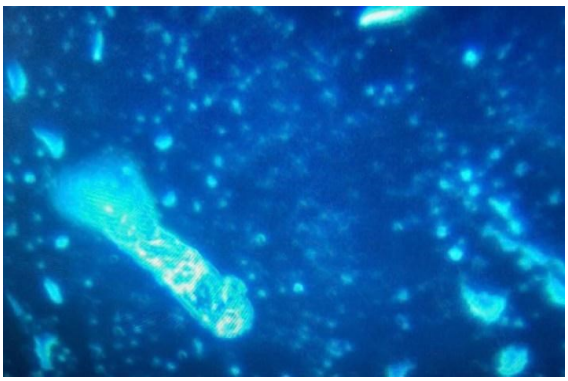

Figure 12. At the poles of the figure (120x magnification) we can see an initial lamellar configuration with crystalline scales resembling structures peculiar to graphene particles.

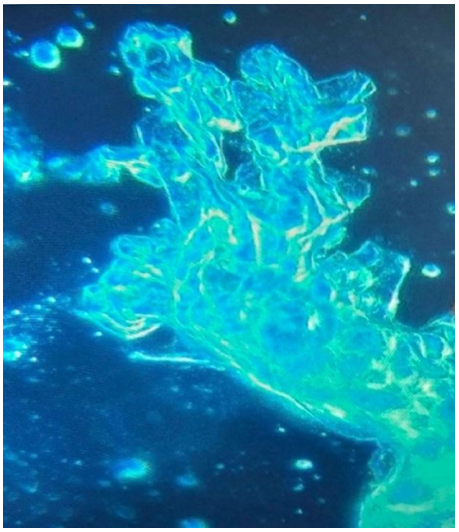

Figure 13. Again, at 120x magnification, geometric figures tend to take shape in extremely complex aggregates.

Biosignaling systems that were formerly under control prior to the mRNA injection(s) are soon compromised by a flood of confusion and biological disinformation (what some have been calling "biosemiotic entropy"; see Pellionisz, 2012; Gryder et al., 2013; Davidson et al., 2013; Shaw, 2017 and their references). As a result, the clinical terrain that was formerly manageable is suddenly fraught with unfamiliar perils never before encountered. For this patient the story of her blood transformations appears in Figures 10 through 18. Before her inoculation with the experimental mRNA concoction her erythrocytes looked normal and healthy as seen in Figure 10(a). But that healthy condition was suddenly changed with the second dose of the Pfizer mRNA injection when her blood profile changed to the pictures seen in Figure 10(b) and 10(c).

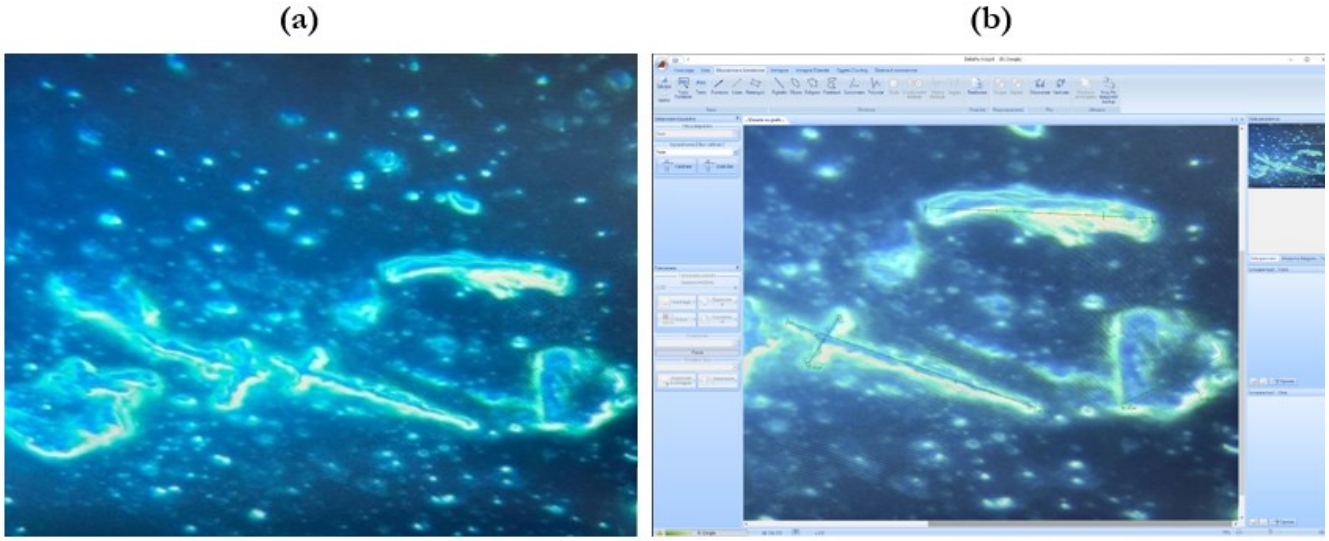

Figure 14. The photos (a) and (b), both at 120x magnification, show tubular, flake, crystalline and mixed shapes configurations, surrounded by clustered fibrin. (Measurement: 146,72µm X 31,03µm - 62,00µm X 61,59µm Delta-Pix Software).

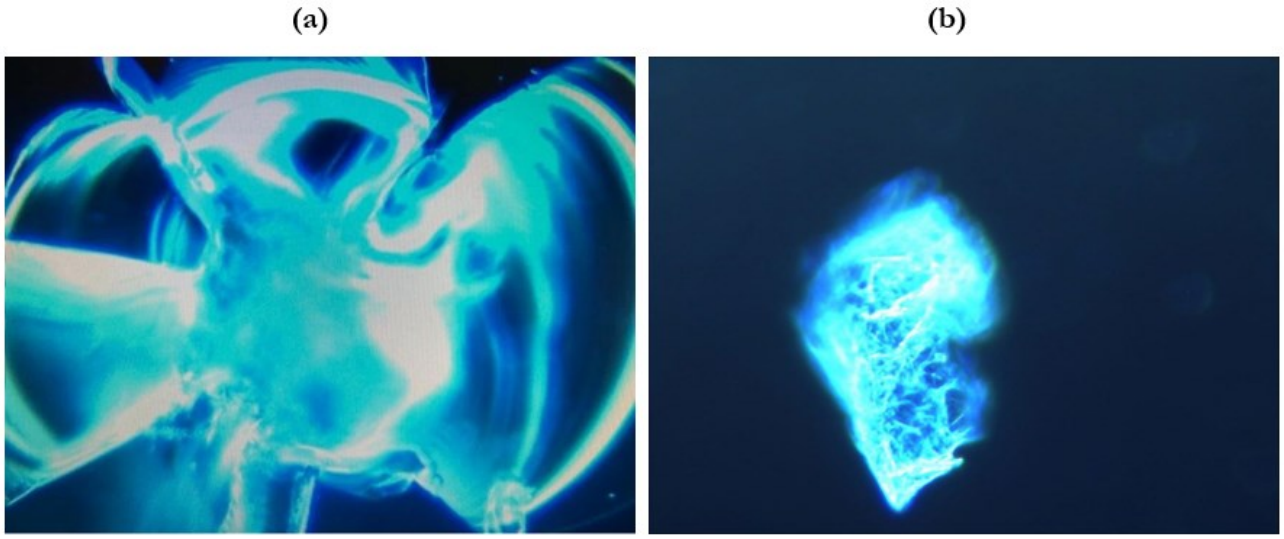

Figure 15. Here are some very smooth and complex crystalline configurations at 120x magnification.

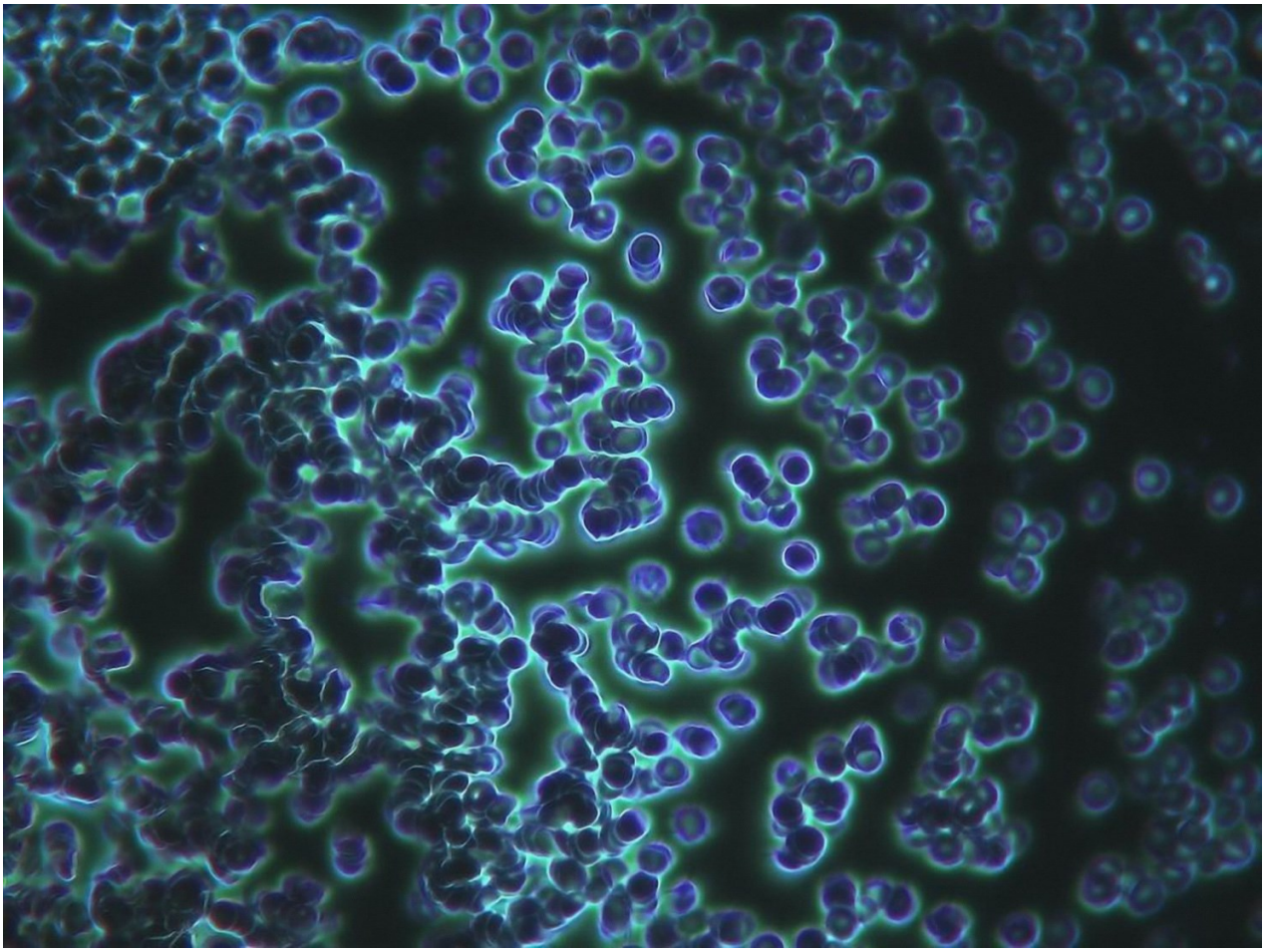

Figure 16. This image, at 40x magnification, is extremely representative of the "Z potential" disorders, with aggregation and "rouleaux stacking" of red blood cells.

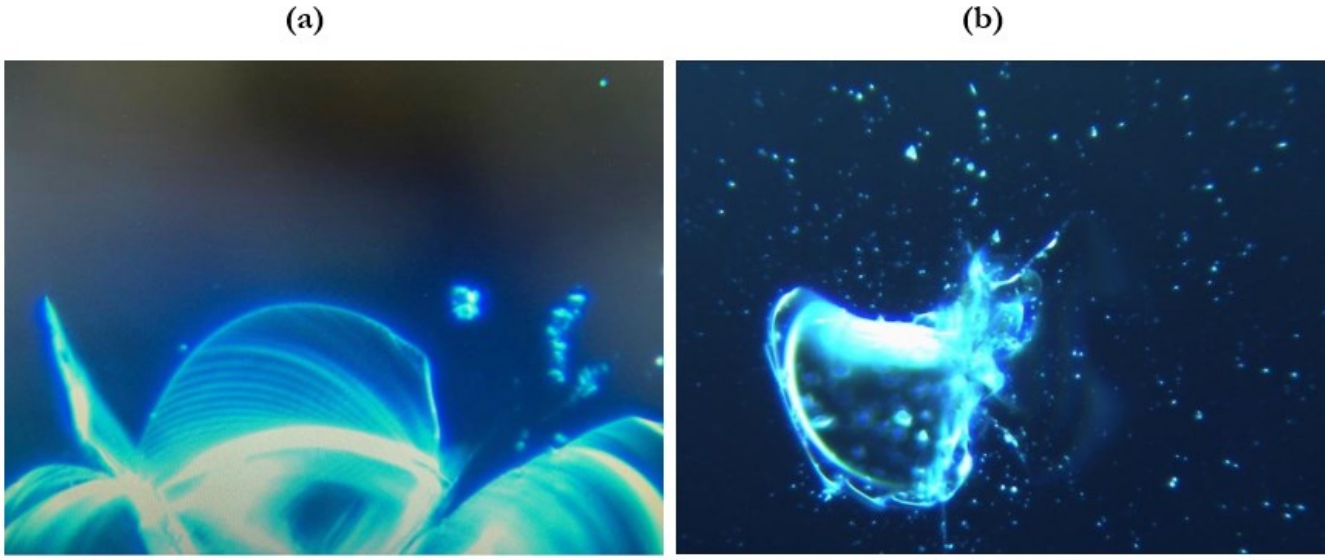

Figure 17. An example of the complex and structured crystal/lamellar organization at 120x magnification. In the picture on the right side a "module" from the morphology and recurrent structuring occurring with great frequency. The aggregating forces are guided by the negative entropic context.

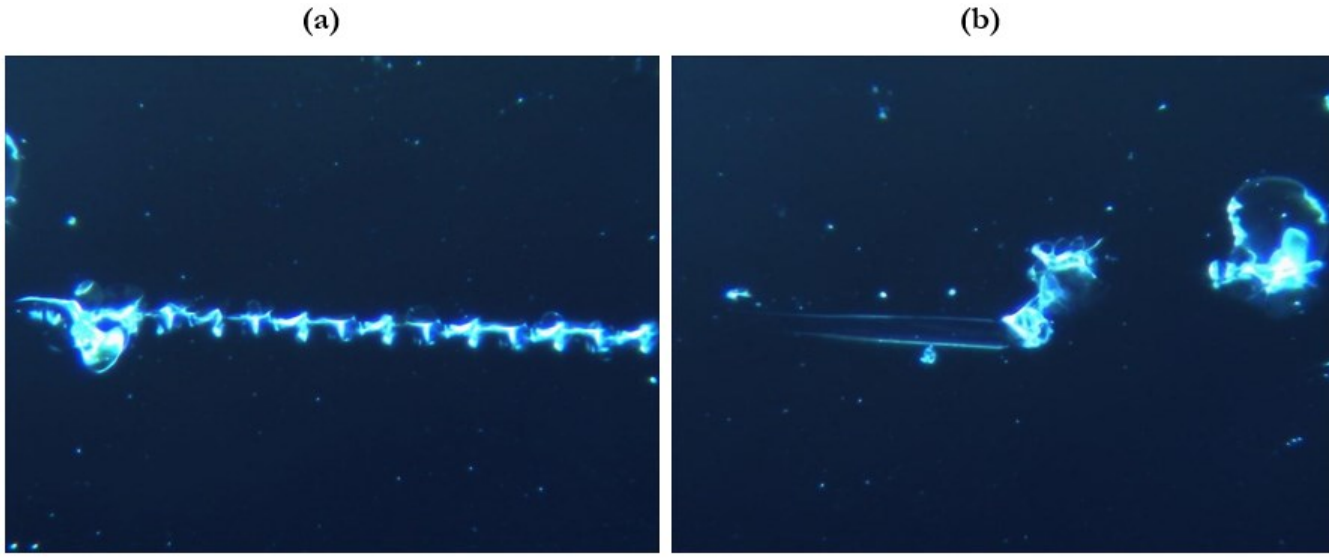

Figure 18. Images of crystalline aggregation, regular and modular, with apparent "self-similar attitudes of fractal nature".

CASE NO. 4 (FIGURES 19-28)

This patient was a 64-year-old male, himself a medical doctor in good health, able to practice martial arts (Ars dynamica CM) involving, among other physical challenges, phases of prolonged apnea (being choked). He was diagnosed with hepatitis A at the age of 10, had a semi-block of the right branch, documented during military service, an episode of benign paroxysmal positional vertigo at the age of 30, with recurrence

at 54 and 60 years of age. To comply with the anti-COVID harassment for medical clinicians, on 17 December 2021 he had the first dose of the Moderna mRNA concoction. In the following period, significant episodes of tachyarrhythmia were treated with 3 sessions of pulsed electric field. After relapse of paroxysmal positional vertigo (treated with a pulsed magnetic field), he had a peripheral blood test taken which identified the structures that seem likely to be graphenic particles. On January 30, 2022, the patient's smear was re-evaluated, after having taken the second dose of Moderna on January 28. The configurations of the foreign particulate, presumably graphenic particles, were very evident as can be seen in Figures 19 through 28. From the clinical point of view, blood hyper-coagulability was recorded on the bleeding test; this occurred in a patient who had been rejected from a trial on ticlopidine as suffering from platelet aggregation deficiency (in a trial performed at the Pavia University in 1983) with the advice to use platelet anti-aggregants with caution.

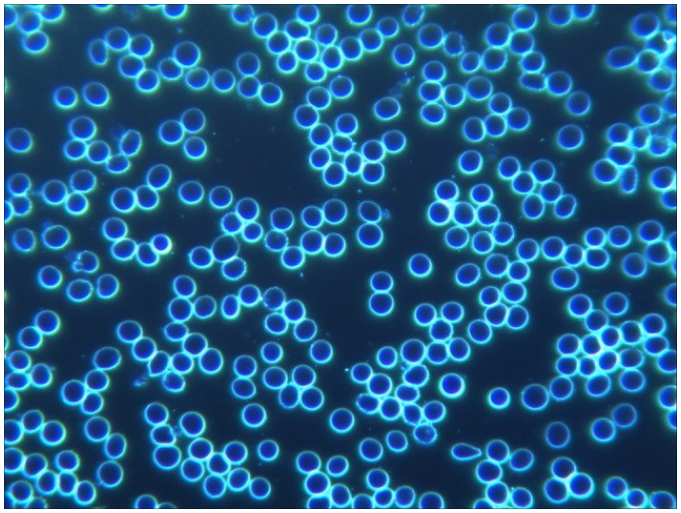

Figure 19. This image at 40x magnification shows the patient's smear before the first dose of the Moderna mRNA injection.

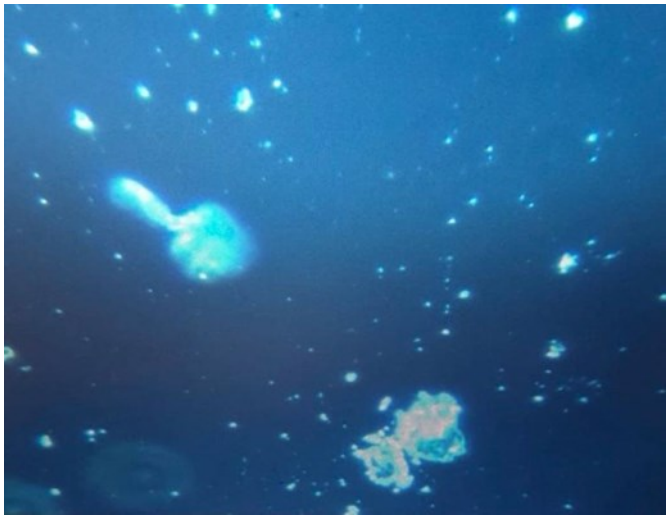

Figure 20. Image at 120x magnification obtained three weeks after the first dose of the Moderna mRNA concoction: structures appear in dispersed and initially conglobate configuration

Although the patient had taken 500 mg of aspirin daily for a week, it was not possible to obtain a blood sample from the scarification site. The same problem arose during the finger prick sampling, for the second fresh blood test, when previously he would bleed for hours for example after shaving. Currently the patient has severe, a persistent and disabling headache, loss of concentration and difficulty in performing even routine professional activities, bilateral tinnitus, an arrhythmic heartbeat, and tachycardic crises. The patient was taking Prisma, a 50 mg tablet per day, cardio-aspirin, Vitamin D3 4,000 U.I. per day, and was receiving Pulsed Electrostatic Therapy in 3 sessions each week. For this person, Figures 19 through 28 tell the story of his changing blood profile going from normal to very abnormal.

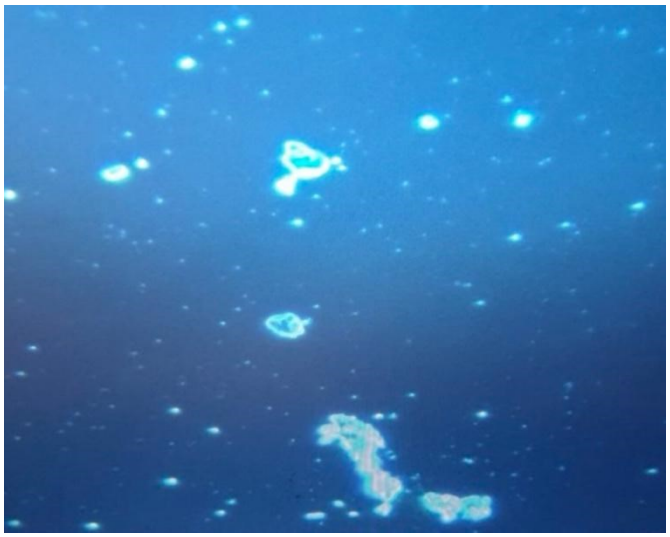

Figure 21. Another image at 120x magnification taken three weeks after the first dose of Moderna.

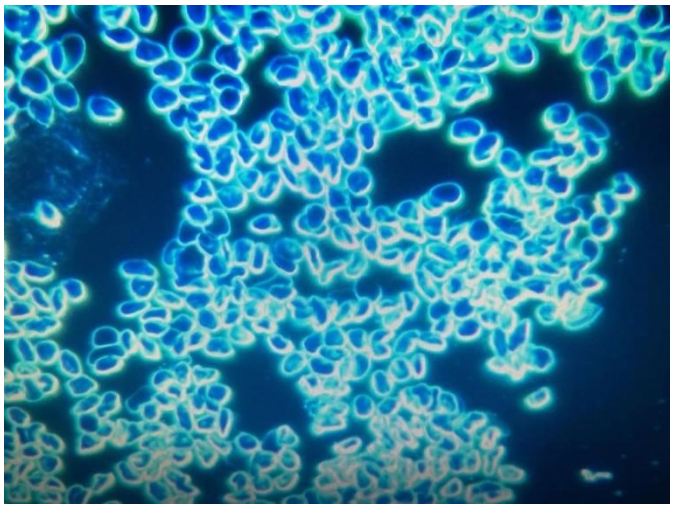

Figure 22. Image at 40x magnification showing aggregation and morphological modification of the erythrocytes two days after the second dose of a Moderna mRNA injection.

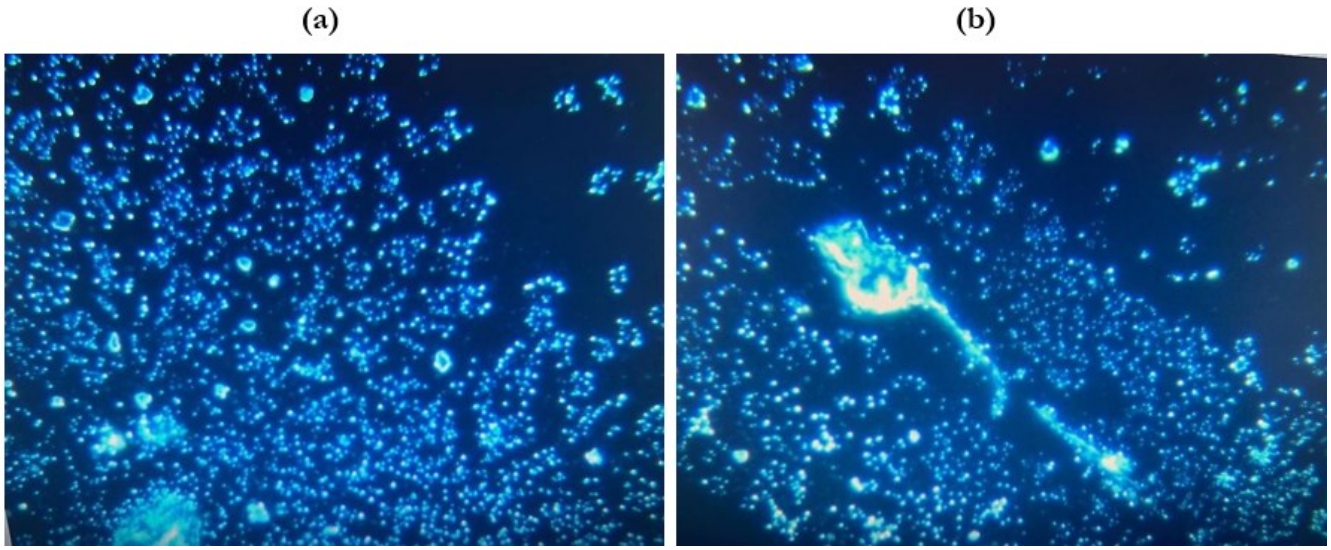

Figure 23. Illustrative images (a) and (b) at 120x magnification showing the different types of aggregations taking shape.

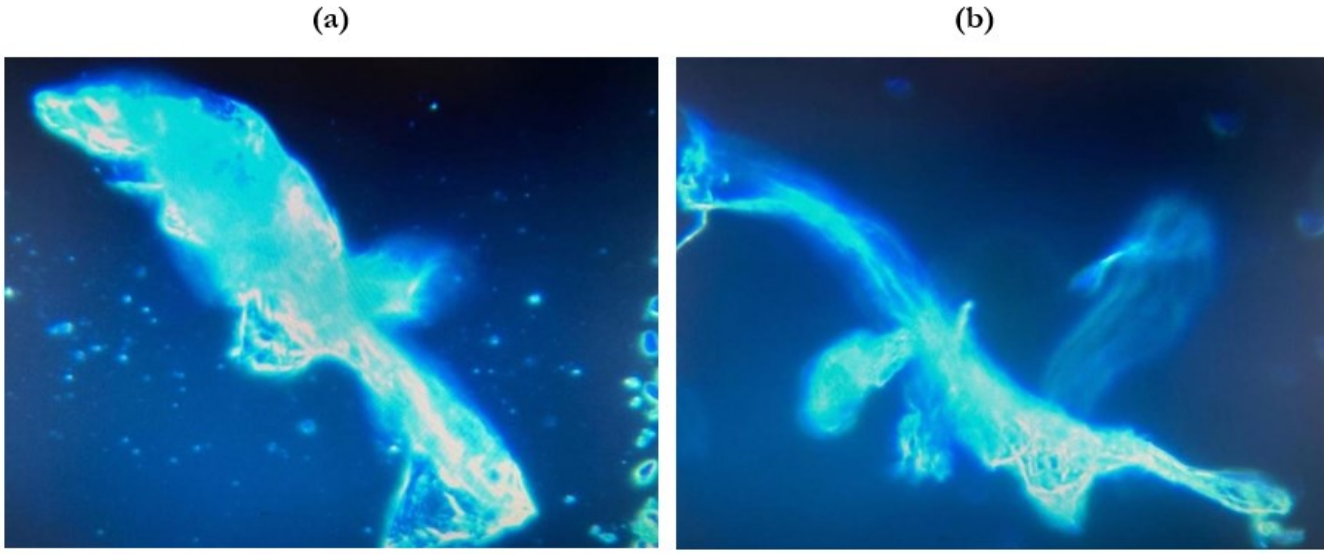

Figure 24. Evident tubular formations at 120x magnification in the aggregative phase showing their complex morphology.

Figure 25. Here at 120x magnification (3x magnification digitally produced) (a) and (b) show tubular formations that seem to be in different aggregative stages.

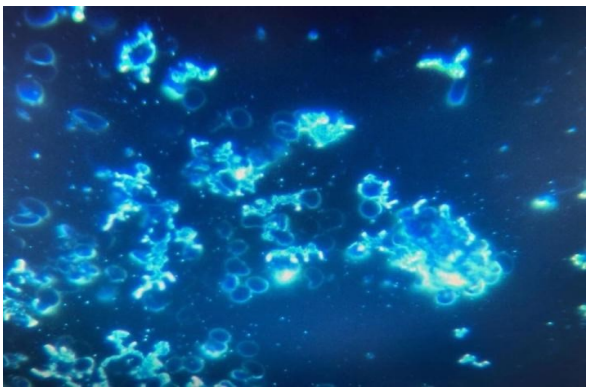

Figure 26. In this image at 40x magnification, it seems that the red blood cells are being adsorbed on particulate structures.

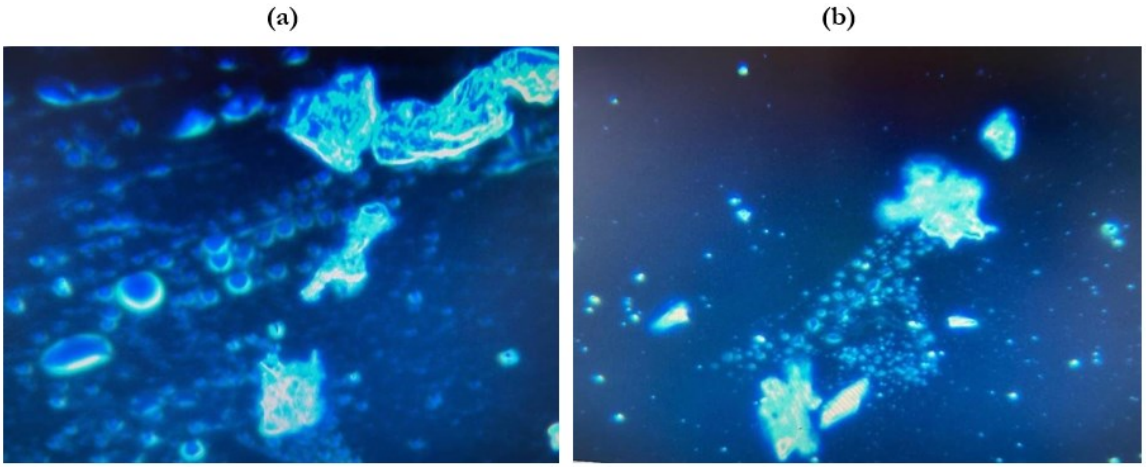

Figure 27. In these images at 40x magnification erythrocyte seem to be drawn towards the conglomerates.

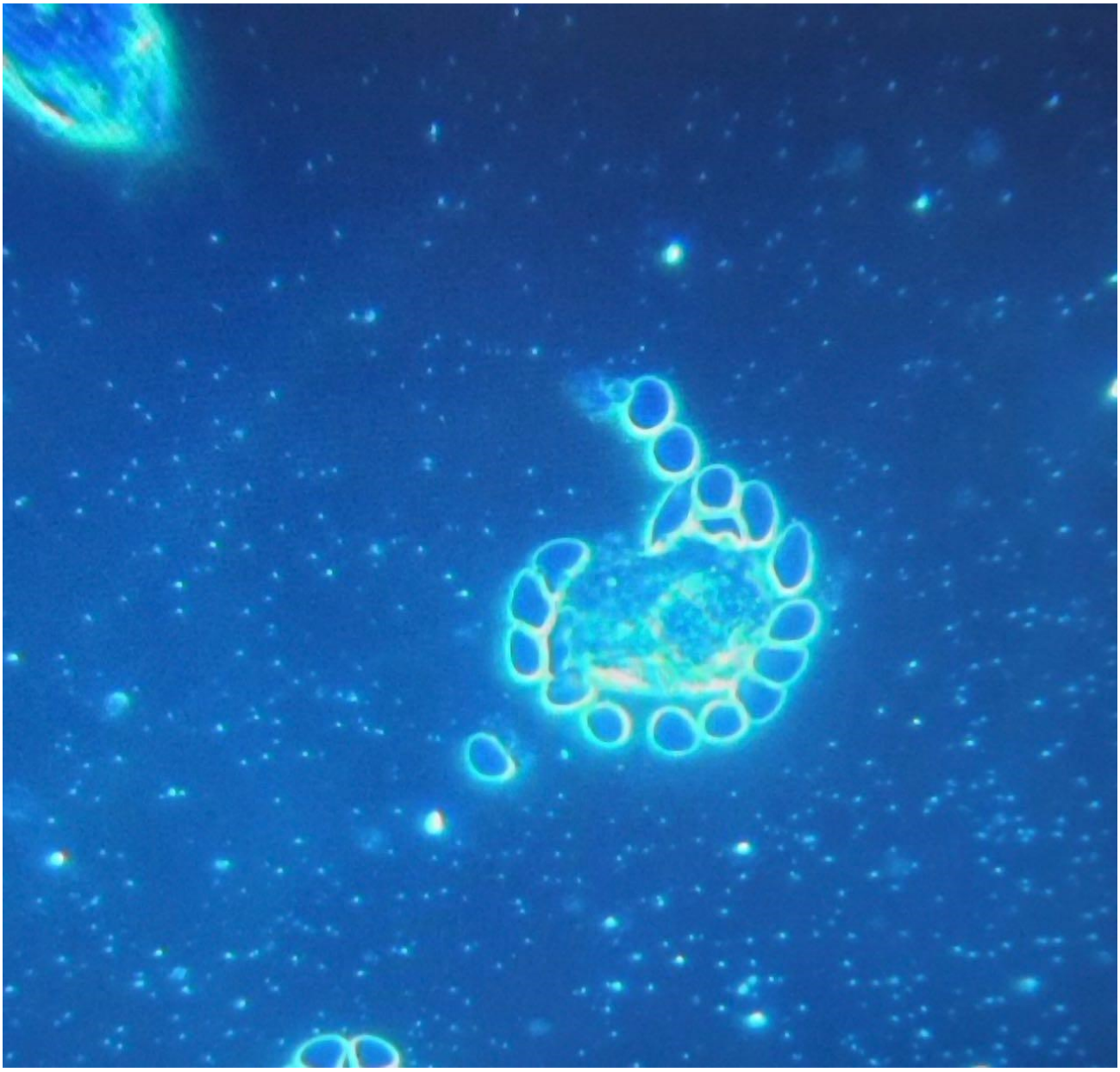

Figure 28. This photograph at 40x magnification highlights the interface of the interaction between red cells and what is presumably a graphenic particle.

DISCUSSION AND CONCLUSIONS

In the present study, blood samples of 1,006 symptomatic subjects after one or more anti-COVID mRNA injections from Pfizer/BioNTech or Moderna were analyzed under an optical microscope in the dark-field. Of the 1,006 cases, 948 (94.23%) showed various alterations in their blood. Aggregation of erythrocytes were highlighted and exogenous point-like and self-luminescent particles in the dark-field were detected. The luminescence of those particles was markedly higher than that of oxygenated red blood cell walls. The particulate infiltrates, whatever they may consist of, gave the appearance of a starry sky at night. All of the

abnormal blood samples of injected persons, the 948 cases, showed tubular/fibrous formations and frequently also crystalline and lamellar formations with extremely complex but consistently similar morphologies across all of the patients with abnormal blood samples. Our results are so similar to those of Lee et al. (2022) that it could be claimed that, except for our innovative application of dark-field microscopy to mark the foreign metal-like objects in the blood of mRNA injections from Pfizer or Moderna, we have replicated the blood work of the Korean doctors with a much larger sample. Our findings, however, are bolstered by their parallel analysis of the fluids in vials of the mRNA concoctions alongside centrifuged plasma samples from the cases they studied intensively. What seems plain enough is that metallic particles resembling graphene oxide and possibly other metallic compounds, like those discovered by Gatti and Montanari (Montanari & Gatti, 2016; Gatti & Montanari, 2012, 2017, 2018), have been included in the cocktail of whatever the manufacturers have seen fit to put in the so-called mRNA "vaccines". In our experience as clinicians, these mRNA injections are very unlike traditional "vaccines" and their manufacturers need, in our opinions, to come clean about what is in the injections and why it is there.

The blood tests of 12 subjects, carried out with the same methodology before they received any mRNA injections, showed perfectly normal hematological features as documented with the 4 exemplary cases selected from among those 12 to represent all 948 of the abnormal samples we examined. The alterations found after the injection of our patient/cases with mRNA materials (whatever may be in them), we found what we believe is conclusive evidence that the modifications observed, as these persons went from normal blood profiles to very abnormal ones, must be attributed to the proximate mRNA injections.

We assert unequivocally that the 4 cases described in this series are representative of the 948 cases in which extraordinarily anomalous structures and substances were found. The alterations in the erythrocytes show a tendency to aggregation/disintegration, stacking in rouleaux, hemolysis, and other conditions suggestive for an important alteration of their zeta potential (Davidson et al., 2013; Shaw et al., 2014; Davidson & Winey, 2021). Furthermore, there is a well-known tendency for fibrin to cluster that was documented in the biomedical research long ago. These alterations are likely, in our opinions, if not certain, to be involved in producing the coagulation disorders commonly reported after anti-COVID injections (Long et al., 2020; Liu et al., 2021; Seneff et al., 2022). There is also the known vascular toxicity of the spike protein itself (Lei et al., 2021; J. Liu et al., 2021), the principal factor in mRNA injections (Nance & Meier, 2021) and one of the adverse effects in some of the subjects inoculated with mRNA vaccines (Long et al., 2020; Aldén et al., 2022; Trougakos et al., 2022).

With the hematological pictures we have presented here it is reasonable to expect reactivation of oncological disease along with blood circulation disorders. Nearly two decades ago, Miller et al. (2004) showed that disruption of the coagulation pathway was associated with a higher incidence of malignancies. With that research in mind, the observed abnormalities already found in our micrographs of individuals injected with one or more of the experimental mRNA concoctions of Pfizer or Moderna, can no doubt be attributed in part to the foreign materials some of which we suspect are graphene-family particles. These have been observed by many other expert researchers who have examined the so-called "mRNA vaccines". What appear to be graphene based technological composites of some sort have been widely discussed by competent researchers including Armin Koroknay (2021), Pablo Campra (2021), Robert O. Young (2021), the distinguished group of New Zealand Doctors Speaking Out with Science (NZDOS, 2022), Andreas Noack (2022), and others. All these doctors and researchers have also examined the actual contents of the so-called SARS-CoV-2 "vaccines". Additionally, Lee et al. (2022) showed that the strange particulated matter found in the Pfizer and Moderna mRNA injections, also appeared in centifuged blood plasma from recipients of those injections. Such graphene-family materials have been intensively studied by researchers

for decades and increasingly so since COVID-19. A Web of Science search for "graphene AND covid" produced 190 hits and "graphene AND vaccine" turned up 124 hits on July 30, 2022. However, a search for "graphene oxide" generated 133,756 dating from 1995 to the present. Taking account of the findings of Ou et al. (2016), showing that "graphene-family nanomaterials" have been associated with "physical destruction, oxidative stress, DNA damage, inflammatory response, apoptosis, autophagy, and necrosis" on account of their stressful impact on "toll-like receptors- . . . , transforming growth factor β- (TGF-β-) and tumor necrosis factor-alpha (TNF-α)", if the mRNA concoctions by Pfizer and Moderna do contain the suspected graphene materials, they are implicated as disease causing in the recipients of those vaccines.

A second factor known to be involved in disruption of complex biosignaling at the post-translation level of protein production is the supposedly "safe and effective" artificial mRNA concoction aiming to produce the SARS-CoV-2 spike protein in the injection recipients. The coding sequence for that spike component was detailed and praised by Nance and Meier (2021) who said that its artificial modifications "cloak mRNA vaccines from the immune system" (p. 753) and supposedly cause the mRNA injected to persevere in producing one spike protein after another by somehow evading the microRNAs that normally regulate the disassembly of the mRNA soon after the protein is produced. But that is not supposed to happen, according to Nance and Meier with the mRNA in Pfizer and Moderna. They suppose the artificial mRNA in those concoctions, containing "the modified nucleobase N1-methylpseudouridine (m1Ψ)" in the place of the normal Uracil, in addition to hiding them from the normal immune functions of the body will "increase their stability" (p. 749), their "protein production" (p. 751), "their half-life" (p. 752), while "decreasing TLR3 activation" (p. 751) on account of the cloaking modifications.

If they are correct in their claims, the research of Palzer et al. (2022) concerning the special role of "the RNA-binding protein KH-type splicing regulatory protein (KSRP)" must be taken into consideration. According to Palzer et al. the KSRP regulatory protein "controls the mRNA stability . . . by initiation of mRNA decay and inhibition of translation, and by enhancing the maturation of microRNAs" (p. 1). Then note that "KSRP-mediated mRNA decay of pro-inflammatory factors is necessary . . . for the induction of robust immune responses. . . . In cancer, KSRP has often been associated with tumor growth and metastasis" (p. 1). It follows that if the mRNA of the Pfizer and Moderna injections merely do what Nance and Meier claim, they must interfere with KSRP and its post-translation regulatory functions which would seem likely to cause reduction of immune functions and greater likelihood of new or recurrent tumorigenesis.

Taken together, the toxic blood clotting impact of graphene-family nanoparticles and whatever other particulate matter may be causing clotting, along with the disruptive influence of the modified mRNA producing SARS-CoV-2 spike protein in a manner interfering with the KSRP splicing reulatory protein, would it be unreasonable to suppose that the sudden onset of physical and mental senility (marasma) seen in our Case No. 4 was probably directly caused by the Moderna injections?

In conclusion, such abrupt changes as we have documented in the peripheral blood profile of 948 patients have never been observed after inoculation by any vaccines in the past according to our clinical experience. The sudden transition, usually at the time of a second mRNA injection, from a state of perfect normalcy to a pathological one, with accompanying hemolysis, visible packing and stacking of red blood cells in conjunction with the formation of gigantic conglomerate foreign structures, some of them appearing as graphene-family super-structures, is unprecedented. Such phenomena have never been seen before after any "vaccination" of the past. In our collective experience, and in our shared professional opinion, the large quantity of particles in the blood of mRNA injection recipients is incompatible with normal blood flow especially at the level of the capillaries. As far as we know, such self-aggregation phenomena have only been

documented after the COVID-19 mRNA injections were first authorized, then, mandated in some countries, and now are still being widely distributed in more than 12.3 billion doses (Bloomberg.com, 2022). Further studies are needed to determine the precise nature and purposes of the foreign particles found in the blood drops of about 94% of the mRNA recipients we have studied. Where do they come from and why are they in these injections?[1]

Funding and conflicts of interest

All Authors declare that they have not received any funding to influence what they say here. They have no conflicts of interest.

They also state that the research reported in their work was carried out in accordance with the Helsinki Declaration of 1964, and that, although all reported data are anonymous, informed consent was obtained from all participants prior to their enrollment in this study.

REFERENCES

Aldén, M., Olofsson Falla, F., Yang, D., Barghouth, M., Luan, C., Rasmussen, M., & De Marinis, Y. (2022). Intracellular reverse transcription of Pfizer BioNTech COVID-19 mRNA vaccine BNT162b2 in vitro in human liver cell line. *Current Issues in Molecular Biology*, *44*(3), 1115–1126. https://www.mdpi.com/1467-3045/44/3/73/htm?s=09

Bloomberg.com. (2022, July 6). More Than 12.3 Billion Shots Given: Covid-19 Tracker. *Bloomberg.Com*. https://www.bloomberg.com/graphics/covid-vaccine-tracker-global-distribution/

Campra, P. (2021, June 28). *Graphene oxide detection in aqueous suspension: Observational study in optical and electron microscopy.* https://www.docdroid.net/rNgtxyh/microscopia-de-vial-corminaty-dr-campra-firma-e-1-fusionado-pdf

Davidson, R. M., Lauritzen, A., & Seneff, S. (2013). Biological water dynamics and entropy: A biophysical origin of cancer and other diseases. *Entropy*, *15*(9), 3822–3876. https://doi.org/10.3390/e15093822

Davidson, R. M., & Winey, T. R. (2021). Vitamin C Mitigating and Rescuing from Synergistic Toxicity: Sodium Fluoride, Silicofluorides, Aluminum Salts, Electromagnetic Pollution, and SARS-CoV-2. *International Journal of Vaccine Theory, Practice, and Research*, *1*(2), 243–282. https://ijvtpr.com/index.php/IJVTPR/article/view/12

Gatti, A. M., & Montanari, S. (2012). Nanoparticles: A New Form of Terrorism? In A. Vaseashta, E. Braman, & P. Susmann (Eds.), *Technological Innovations in Sensing and Detection of Chemical, Biological, Radiological, Nuclear Threats and Ecological Terrorism* (pp. 45–53). Springer Netherlands. https://doi.org/10.1007/978-94-007-2488-4_4

Gatti, A. M., & Montanari, S. (2017). New Quality-Control Investigations on Vaccines: Micro- and Nanocontamination. *International Journal of Vaccines & Vaccination*, *4*(1). https://doi.org/10.15406/ijvv.2017.04.00072

Gatti, A. M., & Montanari, S. (2018). The Side Effects of Drugs: Nanopathological Hazards and Risks. In H. G. Merkus, G. M. H. Meesters, & W. Oostra (Eds.), *Particles and Nanoparticles in Pharmaceutical Products: Design, Manufacturing, Behavior and Performance* (pp. 429–443). Springer International Publishing. https://doi.org/10.1007/978-3-319-94174-5_13

Giovannini, F., & Pisano, G. (in press). Entropia nella gestione clinica di terapie tra biochimica e biofísica [Entropy in the clinical management of therapies between biochemistry and biophysics]. *Medicina Quantistica [Quantitative Medicine]*.

[1] The scanning electron miccroscopy (SEM) analysis with back-scattered electron (BSE) detection, secondary electron (SE) detection, and energy dispersive spectroscopy (EDS) of the blood of two subjects (Cases No. 3 and No. 4), performed by the Electron Microscopy Laboratory, Department of Chemistry, of the University of Turin is to be found in the **ANNEX**.

Gryder, B., Nelson, C., & Shepard, S. (2013). Biosemiotic entropy of the genome: Mutations and epigenetic imbalances resulting in cancer. *Entropy*, *15*(1), 234–261. https://doi.org/10.3390/e15010234

Hidróxido de GRAFENO / Andreas Noack recorded in November 2021. (2022, May 3). https://www.bitchute.com/video/kVvtWhSnc6Eq/

Lee, Y. M., Park, S., & Jeon, K.-Y. (2022). Foreign materials in blood samples of recipients of COVID-19 vaccines. *International Journal of Vaccine Theory, Practice, and Research*, *2*(1), 249–265. https://ijvtpr.com/index.php/IJVTPR/article/view/37

Lei, Y., Zhang, J., Schiavon, C. R., He, M., Chen, L., Shen, H., Zhang, Y., Yin, Q., Cho, Y., Andrade, L., Shadel, G. S., Hepokoski, M., Lei, T., Wang, H., Zhang, J., Yuan, J. X.-J., Malhotra, A., Manor, U., Wang, S., … Shyy, J. Y.-J. (2021). SARS-CoV-2 spike protein impairs endothelial function via downregulation of ACE 2. *Circulation Research*, *128*(9), 1323–1326. https://doi.org/10.1161/CIRCRESAHA.121.318902

Liu, J., Wang, J., Xu, J., Xia, H., Wang, Y., Zhang, C., Chen, W., Zhang, H., Liu, Q., Zhu, R., Shi, Y., Shen, Z., Xing, Z., Gao, W., Zhou, L., Shao, J., Shi, J., Yang, X., Deng, Y., … Liu, Z. (2021). Comprehensive investigations revealed consistent pathophysiological alterations after vaccination with COVID-19 vaccines. *Cell Discovery*, *7*(1), 99. https://doi.org/10.1038/s41421-021-00329-3

Liu, S., Wang, Y., Xu, K., Wang, Z., Fan, X., Zhang, C., Li, S., Qiu, X., & Jiang, T. (2017). Relationship between necrotic patterns in glioblastoma and patient survival: Fractal dimension and lacunarity analyses using magnetic resonance imaging. *Scientific Reports*, *7*(1), 8302. https://doi.org/10.1038/s41598-017-08862-6

Long, H., Nie, L., Xiang, X., Li, H., Zhang, X., Fu, X., Ren, H., Liu, W., Wang, Q., & Wu, Q. (2020). D-dimer and prothrombin time are the significant indicators of severe COVID-19 and poor prognosis. *BioMed Research International*, *2020*, 6159720. https://doi.org/10.1155/2020/6159720

Montanari, S., & Gatti, A. M. (2016). *Nanopathology: The Health Impact of Nanoparticles*. CRC Press.

Nance, K. D., & Meier, J. L. (2021). Modifications in an emergency: The role of N1-methylpseudouridine in COVID-19 vaccines. *ACS Central Science*, *7*(5), 748–756. https://doi.org/10.1021/acscentsci.1c00197

New Zealand Doctors Speaking Out with Science, Burkhardt, A., Lawrie, T., Wakeling, R., Bailey, M., & Baiey, S. (2022). *Micro-Tech in Comirnaty vaccine based on presentation for member of the NZ Health Select Committee and NZ police 22nd March 2022*. https://thebfd.co.nz/wp-content/uploads/2022/06/NZDOS-Presentation-31.-3.22.pdf

Oller, J. W., & Shaw, C. A. (2019). From superficial damage to invasion of the nucleosome: Ranking of morbidities by the biosemiotic depth hypothesis. *International Journal of Sciences*, *8*(06), 51–73. https://doi.org/10.18483/ijSci.2069

Ou, L., Song, B., Liang, H., Liu, J., Feng, X., Deng, B., Sun, T., & Shao, L. (2016). Toxicity of graphene-family nanoparticles: A general review of the origins and mechanisms. *Particle and Fibre Toxicology*, *13*(1), 57. https://doi.org/10.1186/s12989-016-0168-y

Palzer, K.-A., Bolduan, V., Kaefer, R., Kleinert, H., Bros, M., & Pautz, A. (2022). The role of KH-type splicing regulatory protein (KSRP) for immune functions and tumorigenesis. *Cells*, *11*(9), 1482. https://doi.org/10.3390/cells11091482

Pellionisz, A. J. (2012). The decade of fractogene: From discovery to utility—Proofs of concept open genome-based clinical applications. *International Journal of Systemics, Cybernetics and Informatics*, 17–28. http://www.junkdna.com/pellionisz_ieee_hyderabad/

Seneff, S., Nigh, G., Kyriakopoulos, A. M., & McCullough, P. A. (2022). Innate immune suppression by SARS-CoV-2 mRNA vaccinations: The role of G-quadruplexes, exosomes, and MicroRNAs. *Food and Chemical Toxicology*, *164*, 113008. https://doi.org/10.1016/j.fct.2022.113008

Shaw, C. A. (2017). *Neural Dynamics of Neurological Disease*. John Wiley & Sons, Inc. https://doi.org/10.1002/9781118634523.refs

Shaw, C. A., Seneff, S., Kette, S. D., Tomljenovic, L., Oller, J. W., & Davidson, R. M. (2014). Aluminum-induced entropy in biological systems: Implications for neurological disease. *Journal of Toxicology*, *2014*, 491316. https://doi.org/10.1155/2014/491316

Thrilla, J. (2021, August 25). *Toxicology Doctor Armin Koroknay Comparing Non-Vaccinated Blood to Vaccinated Blood After COVID-19 Vaccine Goes Viral*. JordanThrilla. https://www.jordanthrilla.com/post/toxicology-doctor-armin-koroknay-comparing-non-vaccinated-blood-to-vaccinated-blood-after-covid-19-vaccine-goes-viral/

Trougakos, I. P., Terpos, E., Alexopoulos, H., Politou, M., Paraskevis, D., Scorilas, A., Kastritis, E., Andreakos, E., & Dimopoulos, M. A. (2022). Adverse effects of COVID-19 mRNA vaccines: The spike hypothesis. *Trends in Molecular Medicine*, *28*(7), 542–554. https://doi.org/10.1016/j.molmed.2022.04.007

Young, R. O. (2021, February 5). *Scanning & Transmission Electron Microscopy Reveals Graphene Oxide in CoV-19 Vaccines*. Dr. Robert Young. https://www.drrobertyoung.com/post/transmission-electron-microscopy-reveals-graphene-oxide-in-cov-19-vaccines

ANNEX
Scanning Electron Microscopy Analysis of Cases 3 and 4 with Secondary Electron (SE) Detection, Back-Scattered Electron (BSE) Detection, and Energy Dispersive Spectroscopy (EDS)

In this section of our report, we present the following:

Our focus here is on images of foreign entities in the blood samples from Cases 3 and 4 discussed in the main section of our report. Here we look more closely into foreign objects of interest with additional images at different magnifications and with different equipment than used in the main section of our report. Plates 1 and 2 of this Annex report in Italian and English the technical methods used to obtain the images that follow in this supplement to our main report. The images discussed here were obtained with secondary electron detector (SE) of the scanning electron microscope (SEM) to provide more detailed morphological information. In some cases, when we thought it would be useful, we also report images obtained with back-scattered electron (BSE) detection. That technique enables a resolution below 1 nm because of the higher energy of the BSEs. Together with the spectra from energy-dispersive X-ray spectroscopy (EDS/EDX), we are able to learn something about the quantity and distribution of elements in the foreign objects of interest found in the blood of patients who volunteered for this research, the first is one of the authors, and the other, his mother-in-law, both eager to better understand what was circulating in their blood. For each structure of interest, ones that should not be present in blood samples at all, energy-dispersive X-ray spectroscopy (EDS/EDX) was used to obtain point and distribution maps to show the approximate percentages and distribution of the foreign elements. The images presented here are accompanied by some of the standard information supplied by the SEM equipment and its accompanying software (e.g., acquisition parameters such as voltage, magnification, type of detector, and probe current).[2]

[2] For qualified individuals, more information can be obtained by writing directly to the corresponding author.

UNIVERSITÀ DEGLI STUDI DI TORINO
ALMA UNIVERSITAS TAURINENSIS

LABORATORIO DI MICROSCOPIA ELETTRONICA
DIPARTIMENTO DI CHIMICA
Universita' degli Studi di Torino
Via Gioacchino Quarello 15A
10135 Torino

chimica

Torino, 31 marzo 2022

RELAZIONE RIGUARDANTE LE MISURE ESEGUITE CON LA TECNICA DELLA MICROSCOPIA ELETTRONICA A SCANSIONE (SEM) ACCOPPIATA ALLA SPETTROSCOPIA A DISPERSIONE DI ENERGIA (EDS) SU CAMPIONI DI SANGUE

1. OGGETTO
In data 13 febbraio 2022 è pervenuta presso il nostro laboratorio la richiesta di esecuzione di misure con la tecnica della microscopia elettronica a scansione su due campioni di sangue.
Le analisi richieste sono state condotte in data 14 febbraio e 24 febbraio 2022 presso il Laboratorio di Microscopia Elettronica del Dipartimento di Chimica dell'Università degli Studi di Torino sito in via Quarello 15A.
La richiesta del committente era quella di identificare la presenza di strutture aventi morfologie anomale rispetto a quelle, ben conosciute, appartenenti al sangue umano. In particolar modo, la richiesta del committente si fondava sull'identificazione di strutture precedentemente rilevate dallo stesso, con la tecnica della microscopia ottica. Inoltre, una volta identificate, si richiedeva di eseguire l'analisi elementare per individuare la composizione chimica delle stesse.

2. METODOLOGIA ANALITICA
I vetrini da analizzare sono stati preparati subito prima delle analisi tramite striscio e, dopo asciugatura, gli è stato depositato 1 nm di cromo.
La deposizione di un sottile film metallico sul campione si rende necessaria ogniqualvolta si analizzano campioni non conduttivi che impedirebbero l'acquisizione delle immagini. La scelta del cromo è stata necessaria in quanto possiede una grana molto fine adatta per operare con strumentazioni sofisticate come quella utilizzata per l'esecuzione delle misure.

2.1 Principi della Tecnica
La tecnica della microscopia elettronica a scansione (SEM) è una tecnica che utilizza un fascio di elettroni accelerato per produrre delle immagini tridimensionali di un campione. Questa tecnica rappresenta uno strumento indispensabile nell'ambito della caratterizzazione dei materiali e, come tale, viene utilizzata in ogni ambito della ricerca e dell'industria.
Di seguito riporto brevemente alcuni cenni della tecnica in quanto possono essere utili per comprendere meglio l'origine delle immagini prodotte.
Il fascio elettronico prodotto da una sorgente viene opportunamente accelerato e attraversa una serie di lenti elettromagnetiche per essere, finalmente, focalizzato sul campione. Quando gli elettroni del fascio colpiscono il campione, possono avvenire degli urti che daranno origine ad un *volume di interazione* (avente forma a goccia) dal quale fuoriusciranno i segnali utili per produrre le immagini.
I principali tipi di segnali che si originano e che vengono raccolti da opportuni detector sono:
- Elettroni secondari, sono elettroni del campione che dopo aver subito urti con gli elettroni del fascio vengono espulsi dagli strati più superficiali del campione (poche decine di nanometri) e portano con sé informazioni di tipo morfologico e topografico. Le zone più esposte o aventi un rilievo molto accentuato appaiono più luminose nelle immagini prodotte.
- Elettroni retrodiffusi o backscattered, sono elettroni del fascio (più energetici dei secondari) che dopo aver interagito con i nuclei del campione vengono deviati ed espulsi in superficie. La particolarità di questi segnali è che, arrivando da profondità maggiori del campione (1-2 micron), portano con sé informazioni di tipo composizionale. In particolar modo, la presenza di elementi aventi numero atomico più alto (elementi pesanti) appaiono più luminosi e viceversa per quelli più leggeri.

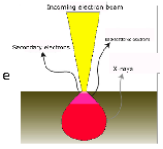

Università degli Studi di Torino _ Codice Fiscale 80088230018– Partita IVA 02099550010

1

Plate 1. Technical description of data obtained on Cases 3 and 4 from the Electron Microscope Laboratory at the University of Torino in the Department of Chemistry on February 13, 2022 reported March 31, 2022.

[English Translation of Plate 1]

Electronic Microscopy Laboratory

Department of Chemistry

University of Turin

Via Gioacchino Quarello 15A

10135 Turin

Turin, March 31, 2022

Report Concerning the Measures Performed with Scanning Electron Microscopy (SEM) Supplemented by Energy Dispersion Spectroscopy (EDS) on Blood Samples

1. Purpose

On February 13, 2022 our laboratory received a request to carry out measures with scanning electron microscopy on two samples of blood. The analysis requested was conducted between February 14 and February 24, 2022 at the Electronic Microscopy Laboratory in the Department of Chemistry at the University of Turin located at Via Querello 15A. The request from the client was to identify structures with anomalous morphology compared to ones well-known in human blood. Specifically, the request from the client was based on their identification of the preceding structures with optical microscopy. Furthermore, once identified, it was requested to pursue the analysis of individual elements to their chemical composition.

2. Analytical Methodology

The slides to be analyzed were prepared immediately before the analysis in strips, and after drying, were treated with 1 nm of chromium. Placing a thin metal wire on the sample is necessary whenever non-conductive samples are analyzed that would [otherwise] prevent the acquisition of the images. The choice of chromium has been necessary as it has a very fine grain suitable for operating with sophisticated instruments such as the one used for the execution of the measures.

2.1 Principles of the Technology

The technology of scanning electron microscopy (SEM) uses an accelerated electron beam to produce a three dimensional image of a sample. This technique is indispensable with respect to characterizing materials and as such is useful in every area of research and of industry. The following briefly offers some facts that may be useful in understanding the origin of the images produced. The electronic bundle produced by a source is appropriately accelerated and crosses a series of electromagnetic lenses that is finally focused on the sample. When the electrons of the bundle hit the sample, shocks can take place that will give rise to a volume of interaction (having a droplet shape) from which the signals useful for producing images will escape by flourescence. The main type of signals that propagate and that are collected by appropriate detectors are:

- Secondary electrons, they are electrons of the sample and after being hit by the band of electrons being expelled from the most superficial layers of the sample (a few dozen nanometers at most) bringing with them morphological and topographical information. The most exposed or very accentuated areas appear brighter in the images produced.
- Retro-diffused, or back-scattered electrons, are electron bundles (more energetic than the secondary electrons) which, after interacting with the sample nuclei, are turned and expelled on the surface. The peculiarity of these signals, arriving from depths greater than the sample (1-2 microns), bring with them compositional information. Specifically, the presence of elements with a higher atomic number (heavy elements) appear more luminous and the opposite is true for the lighter ones.

UNIVERSITÀ DEGLI STUDI DI TORINO
ALMA UNIVERSITAS TAURINENSIS

LABORATORIO DI MICROSCOPIA ELETTRONICA
DIPARTIMENTO DI CHIMICA
Universita' degli Studi di Torino
Via Gioacchino Quarello 15A
10135 Torino

chimica

DOCUMENTAZIONE FOTOGRAFICA

In questo documento viene riportata la raccolta fotografica relativa ai due campioni di sangue analizzati con le tecniche FE-SEM/EDS.

Cosa troverete in questo documento:

- Per ogni «struttura» riscontrata sono state riportate diverse fotografie a diversi ingrandimenti. Le immagini riportate sono state ottenute con il detector per gli elettroni secondari (SE) che, fornendo informazioni di tipo morfologico, sono risultate quelle più utili per il nostro scopo di indagine. In qualche caso, quando ho ritenuto utile, ho riportato anche quelle in BSE.
- Per ogni struttura riscontrata sono state acquisite delle microanalisi (EDS) sia puntuali sia come mappe di distribuzione. Queste informazioni, oltre alla visualizzazione grafica delle mappe, riportano anche le percentuali semi-quantitative degli elementi presenti. Tali microanalisi sono state acquisite in alcune zone dove è stato ritenuto più opportuno.
- Le immagini qui riportate sono corredate di marker, unico dato essenziale che deve essere associato ad un'immagine di microscopia elettronica ma se si desiderasse consultare le immagini «tali e quali come vengono fornite dallo strumento» (cioè, contenenti tutti i parametri di acquisizione : voltaggio, ingrandimento, tipo di detector e corrente di probe) queste si trovano nell'allegato «Materiale di supporto». Inoltre, nello stesso allegato potrete anche consultare le immagini acquisite in modalità BSE (contrasto chimico) che pur non essendo fondamentali in questo caso, sono utile per avere un quadro completo dei campioni analizzati.

Plate 2. Photographic documentation.

[English Translation of Plate 2]

This document shows the photographic collection relating to the two blood samples analyzed with the FE-SEM/DS techniques.

What you will find in this document:

- For each "structure" encountered different photographs were reported with different magnifications. The images reported were obtained with the detector for secondary electrons (ES) which, providing morphological information, proved to be the most useful for our investigation purpose. In some cases, when it seemed useful, those in BSE [back-scattered electrons] were brought back.
- For each structure encountered microanalyses with (EDS [**Energy Dispersion Spectroscopy]**) were acquired both at the site and as distribution maps. This information, in addition to the graphical visualization of the maps, also reports the semi-quantitative percentages of the elements present. These microanalyses have been acquired in some areas where it was considered more appropriate.
- The images here are reported with only the essential data associated with each electron microscope image.

SUMMARY PHOTO DOCUMENTATION

Supplementary Materials

UNIVERSITÀ DEGLI STUDI DI TORINO
ALMA UNIVERSITAS TAURINENSIS

LABORATORIO DI MICROSCOPIA ELETTRONICA
DIPARTIMENTO DI CHIMICA
Universita' degli Studi di Torino
Via Gioacchino Quarello 15A
10135 Torino

chimica

DOCUMENTAZIONE FOTOGRAFICA
SOMMARIO

2

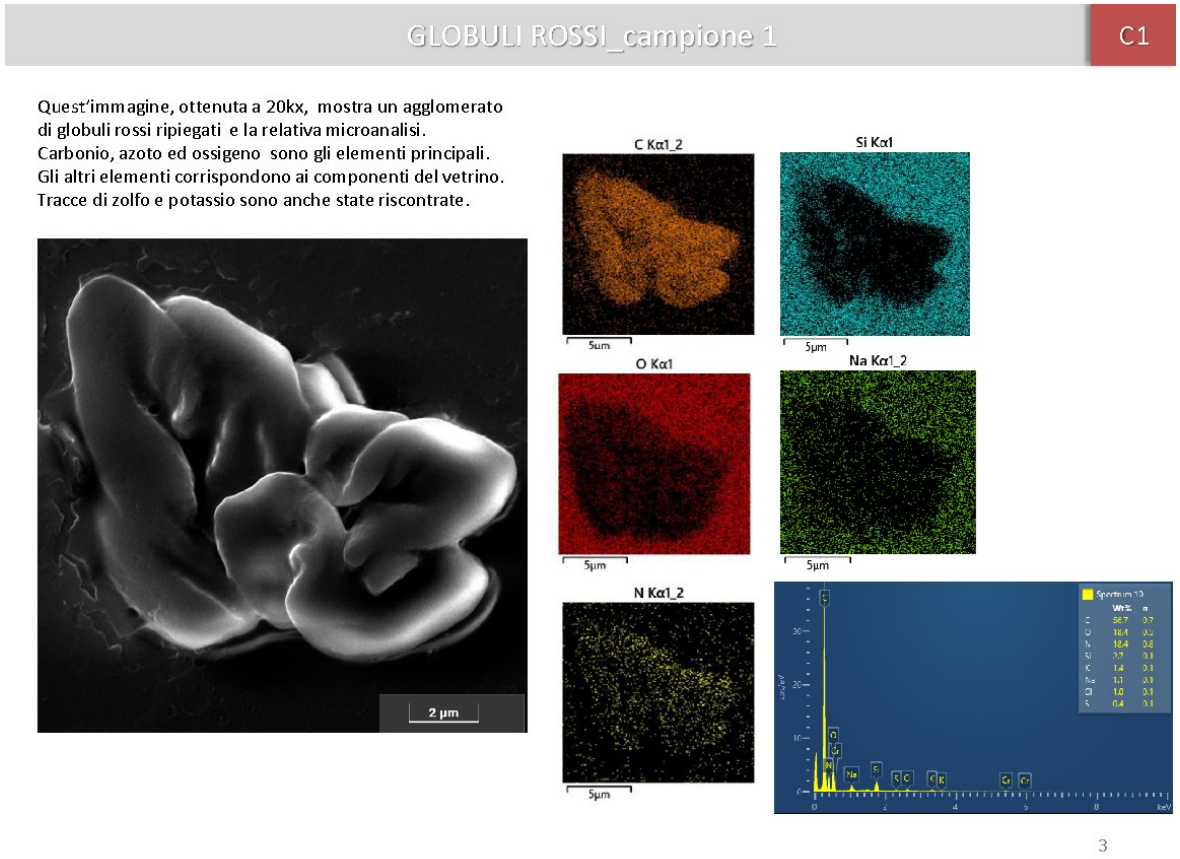

This image obtained at 20 kx, shows an agglomeration of folded red blood cells and its micro analysis. Carbon, nitrogen and the oxygen are the main elements. The other elements correspond to the components of the slide. Traces of sulphur and potassium are also found.

Struttura 1 C1

Le immagini qui riportate sono state acquisite a 8kx e mostrano la presenza di un corpo allungato, ed attorcigliato su se stesso, di lunghezza superiore a 40 micron e spessore variabile di qualche micron.

Entrambe le immagini acquisite (SE&BSE) mettono in evidenza una struttura avente morfologia molto diversa da quella dei globuli.
Per poter studiare meglio la natura di questa struttura si è proceduto con l'acquisizione di immagini ad ingrandimenti maggiori di diverse zone.

SE

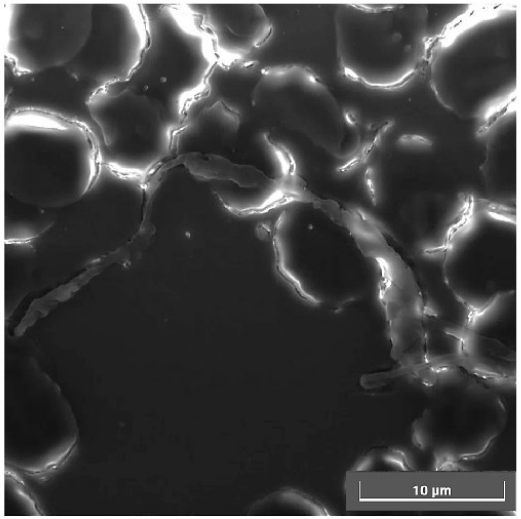

BSE

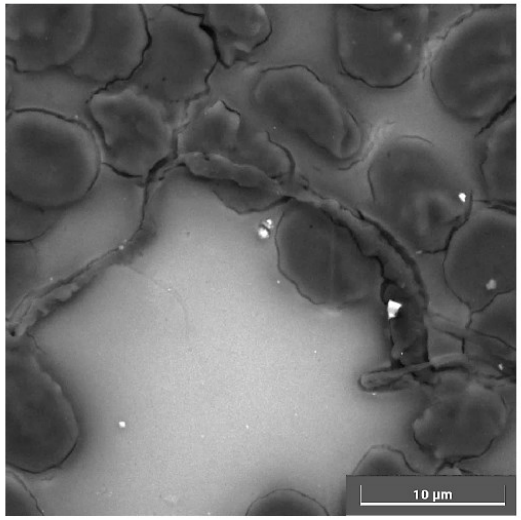

4

The images shown were acquired at 8 kx and show the presence of an elongated, twisted body over 40 microns in length and a variable thickness of a few microns.

Both images (SE&BSE) show a structure with a morphology very different from that of the globules. In order to better study the nature of this structure, we proceeded with the acquisition of images and higher magnifications of different areas.

Le mappe di distribuzione degli elementi dell'area indagata mostrano come il carbonio sia l'elemento preponderante costituente il corpo allungato. La mappa del carbonio, in rosso, mostra infatti un accumulo di questo elemento su tutta la lunghezza. La presenza preponderante di questo elemento è evidente osservando come la mappa relativa sembra una copia della fotografia. Lo stesso non può dirsi dell'ossigeno che, anche se presente, lo è in percentuali ben più basse.
Ho riportato anche la mappa del silicio (costituente il vetrino) come riferimento. Un'informazione molto utile che può essere tratta guardando la mappa del silicio è che, in corrispondenza di una parte del corpo «estraneo» si osserva una zona scura (a destra) . Questo indica che in quella zona, lo spessore del corpo è maggiore rispetto al resto.

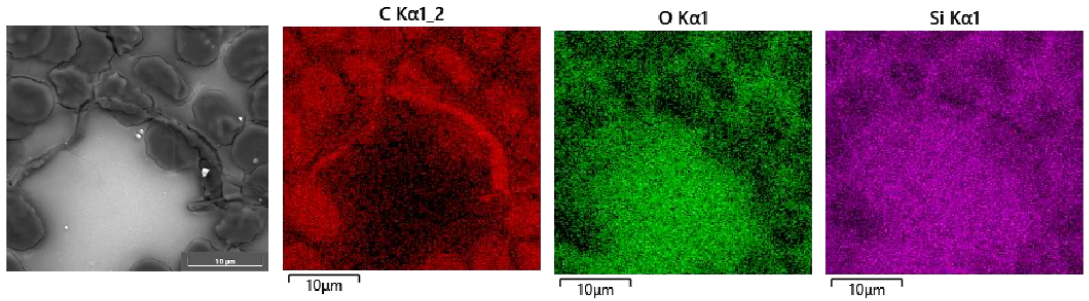

5

The distribution maps of the elements in the investigated area show that carbon is the predominant element constituting the elongated body. The carbon map in red shows an accumulation of this element along the entire length. The predominant presence of this element is evident by observing how the relative map looks like a copy of the photograph. The same cannot be said of oxygen which, although present, is present in much lower percentages. We have also included the map of the silicon (constituent of the slide) for reference. A very useful piece of information that can be gleaned from looking at the silicon map is that there is a dark area (right) corresponding to a part of the "foreign body". That indicates, in this area, the greatest thickness than in the rest of the body.

L'immagine a destra è l'ingrandimento acquisito a 70kx dell'area indicata nel riquadro dove si osservano più strati sovrapposti e stropicciati.

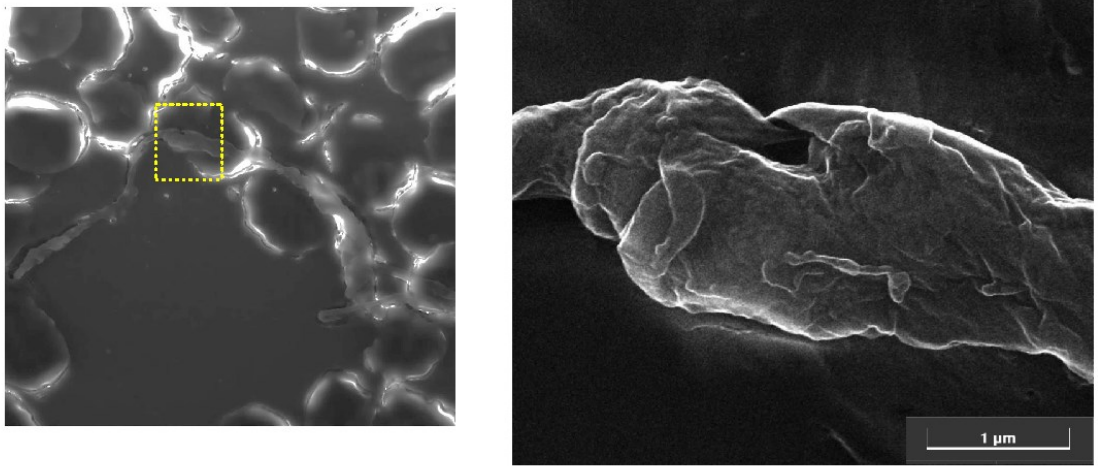

6

The image on the right is an enlargement acquired at 70 kx of the area indicated in the box, where several overlapping and crumpled layers can be seen.

Dettaglio a 70kx C1

Ulteriore ingrandimento acquisito a 70kx di una zona diversa, indicata nel riquadro, dove si osserva nuovamente la presenza di più strati sovrapposti .
In pagina successiva, la microanalisi confermerà ulteriormente la natura, prevalentemente carboniosa della stessa.

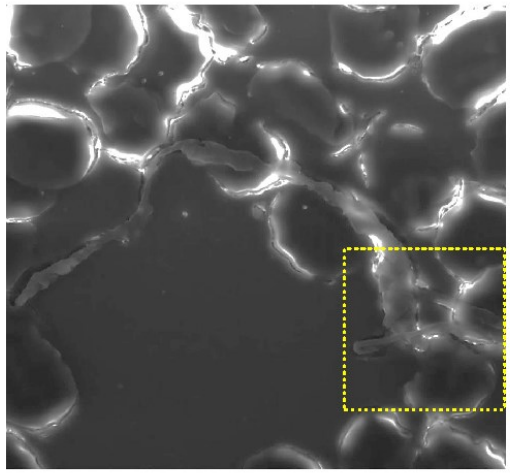

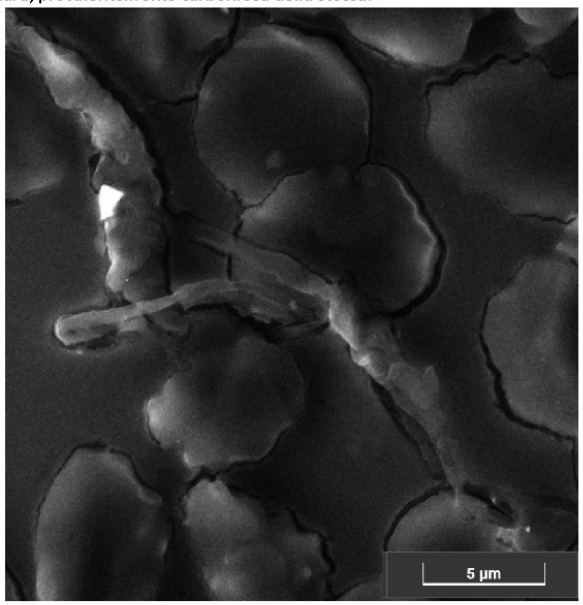

7

Further magnification acquired at 70 kx of a different area, indicated in the box, where the presence of several overlapping layers is again observed.

On the next page, the micro-analysis will further confirm the predominantly carbonaceous nature of the material.

La mappa di distribuzione degli elementi evidenzia l'accumulo di carbonio nella zona corrispondente al corpo in questione.
La mappa del silicio mostra la componente principale del vetrino e può essere utile come riferimento per le altre mappe.

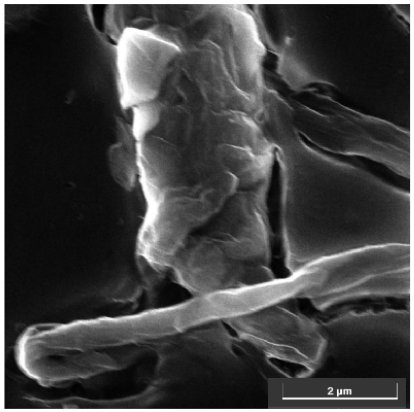

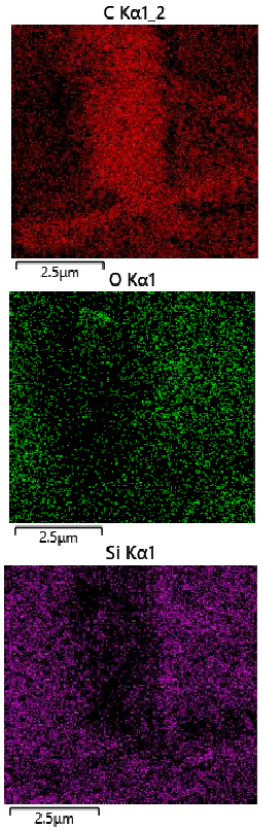

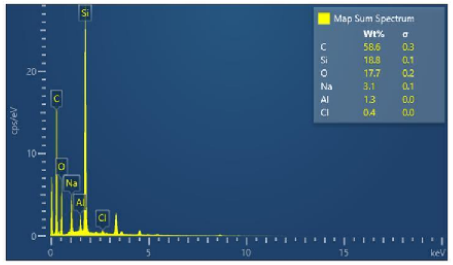

8

The element distribution map shows the accumulation of carbon in the area corresponding to the body in question. The silicon map shows the main component of the slide and can be useful as a reference for the other maps.

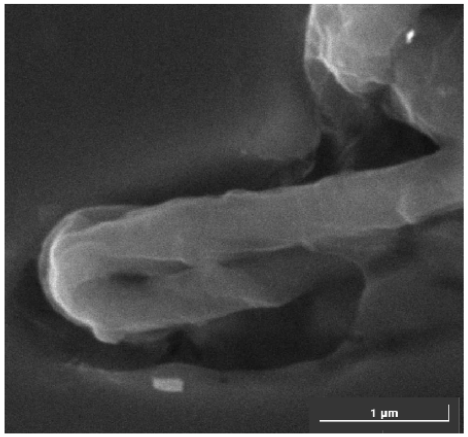

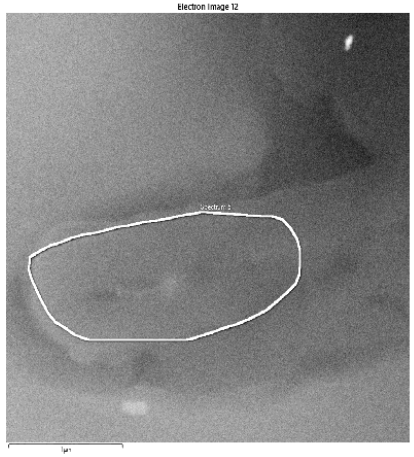

La microanalisi puntuale eseguita sulla zona indicata ha messo in evidenza la presenza di carbonio al 63%. Sono anche stati evidenziati gli elementi costituenti del vetrino (silicio, ossigeno e sodio). Tracce di sali (cloruro di sodio e/o cloruro di potassio) sono anche state rilevate.
Alluminio e silicio possono essere dovuti alla presenza di qualche silicoalluminato (particelle più chiare), componente del particolato atmosferico.

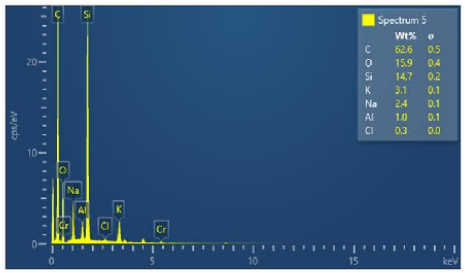

9

The micro point analysis performed on the indicated area revealed the presence of 63% carbon. The constituent elements of the slide (silicon, oxygen and sodium) were also highlighted. Traces of salts (sodium chloride and/or potassium chloride) were also detected.

Aluminium and silicon may be due to the presence of some silicoaluminate (lighter particles), component of atmospheric particulate matter

Dettaglio a 280kx C1

Per finire, l'immagine qui riportata è stata ottenuta ad un alto ingrandimento, 280kx, e mostra la struttura superficiale del film componente questa struttura che ricorda quelle tipiche delle strutture grafeniche.

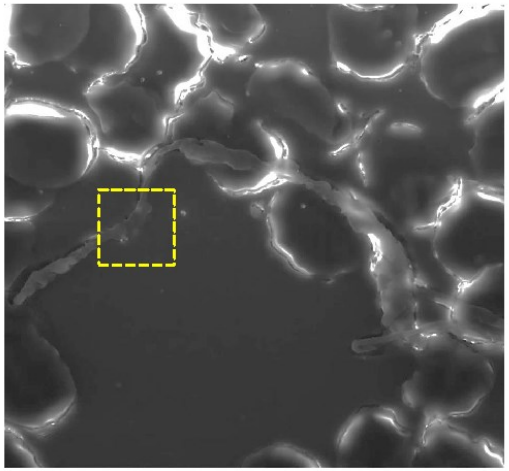

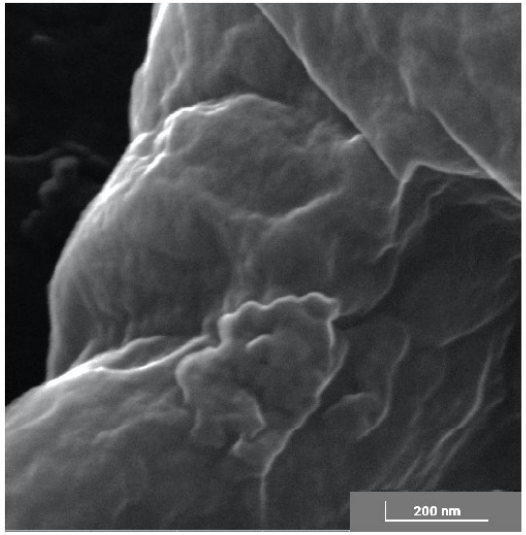

10

Finally, the image shown here was obtained at a high magnification, 280 kx, and shows the surface structure of the component film that resembles those presumably graphenic particles.

Queste immagini, acquisite a 9kx, riportano la seconda struttura riscontrata nel campione 1.
Questa sembra mostrare un globulo rosso infilzato da una struttura di tipo «foglio stropicciato» e ripiegata.
Nella pagina successiva vengono riportate le microanalisi puntuali eseguite sia sulla parte «tondeggainte» sia sul corpo che lo attraversa in modo da valutare le eventuali differenze di composizione elementare anche se. Già guardando l'immagine in BSE si può Prevedere che la composizione sarà molto simile (livelli di grigio molto simili).

SE

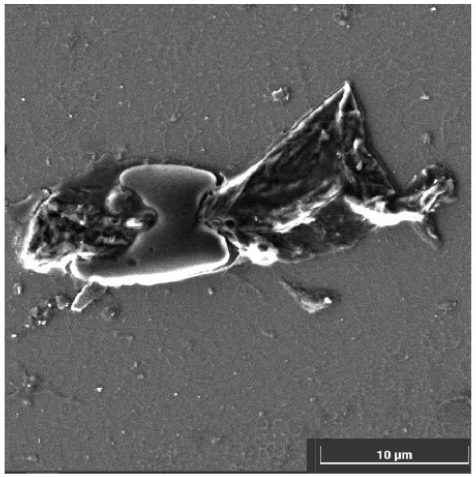

BSE

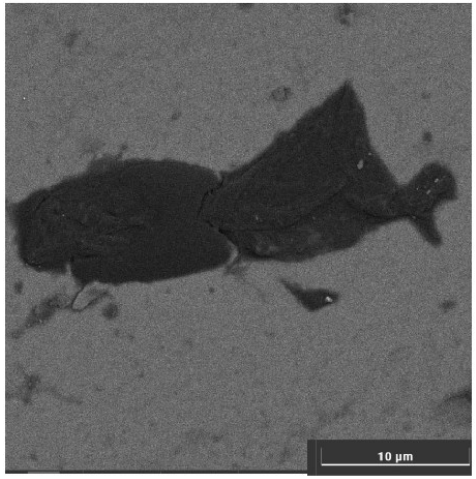

11

These images obtained at 9 kx show the second structure found in sample 1. This seems to show a red blood cell impaled by a "crumpled sheet" and folded structure. The next page shows the precise micro analyzes performed both on the rounded part and on the body that passes through it in order to evaluate any differences in composition, even if already looking at the BSE image it can be expected that the composition will be very similar (levels of gray very similar).

Gli elementi costitutivi il globulo ed il corpo che lo attraversa sono gli stessi: carbonio, azoto ed ossigeno. L'azoto sembra essere maggiormente presente nel globulo.
Il silicio ed il sodio riscontrati nel film (spettro 25) appartengono ai componenti del vetrino che, in questo caso, essendo il film molto sottile, sono stati rilevati.

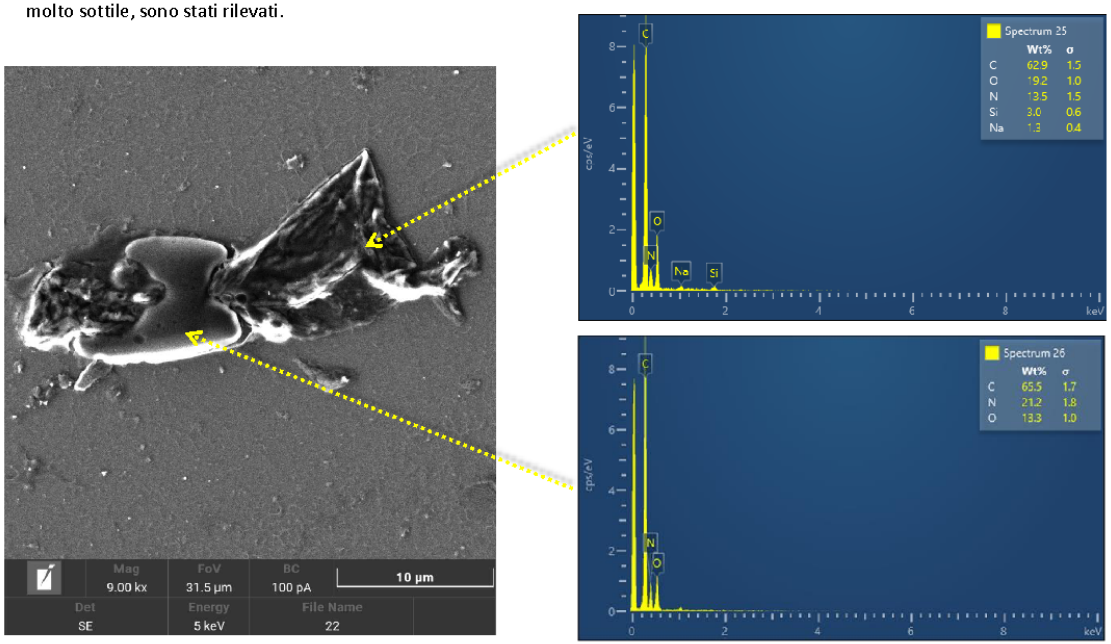

12

The constituent elements of the globule and the body that passes through it are the same, carbon, nitrogen and oxygen. Nitrogen appears to be more present in the blood cell. The silicon and sodium found in the film (spectrum 25) belong to the components of the slide, which in this case, being the film very thin, have been detected.

La mappa di distribuzione degli elementi conferma la prevalente presenza di carbonio con percentuali minori di azoto ed ossigeno.

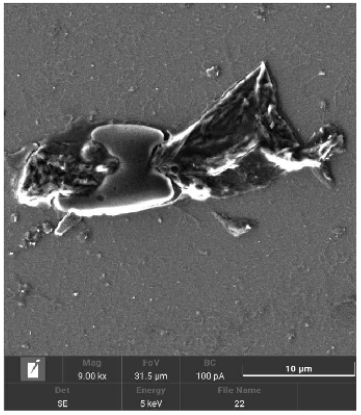

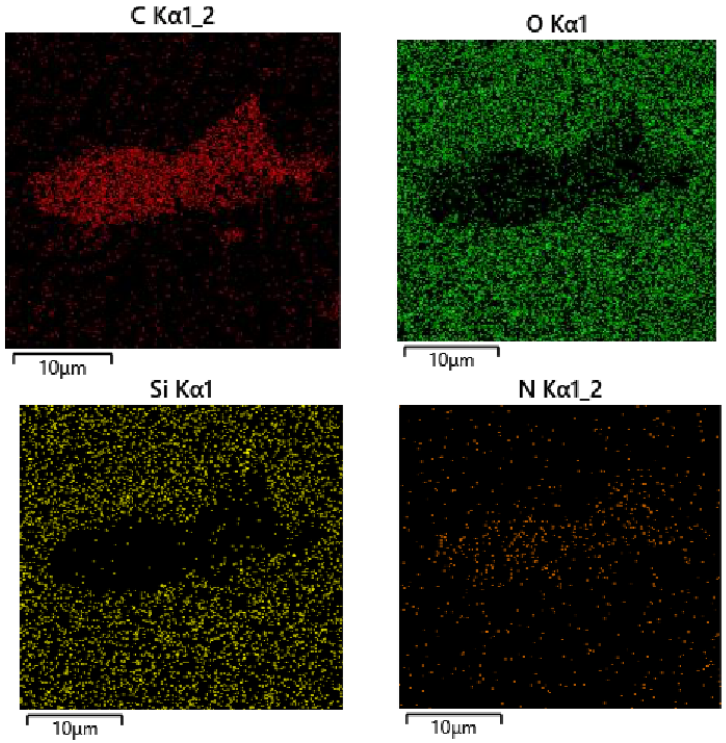

13

The distribution map of the elements confirms the prevalent presence of carbon with lower percentages of nitrogen and oxygen.

Struttura 3 C1

Questa terza struttura riscontrata nel campione 1 mostra due corpi aventi linee geometriche molto ben definite con angoli altrettanto definiti. Le dimensioni di queste strutture sono di qualche decina di micron.
In questo caso, riporto anche le foto in BSE in quanto utili per la visualizzazione dei confini della struttura.
Le immagini in SE mostrano i bordi molto luminosi (caratteristico di questo tipo di segnale) ad indicare che sono corpi con maggiore rilievo topografico. Guardando entrambe le immagini si individua chiaramente come queste due strutture si stacchino dal vetrino di supporto facendo vedere molto bene i bordi regolari. Inoltre, la loro texture appare molto diversa dal resto del campione. Le immagini ad ingrandimenti maggiori, presenti nelle pagine successive, metteranno in evidenza questo aspetto.

SE

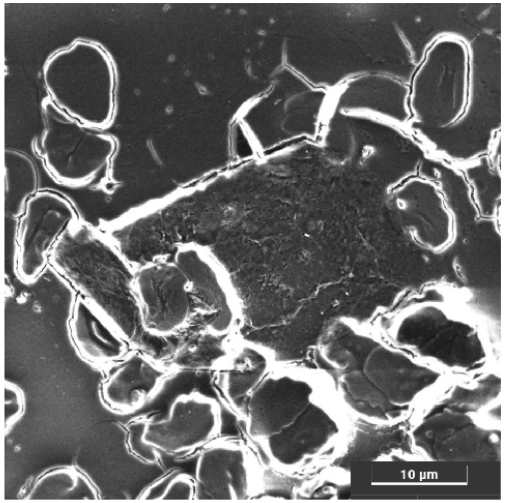

BSE

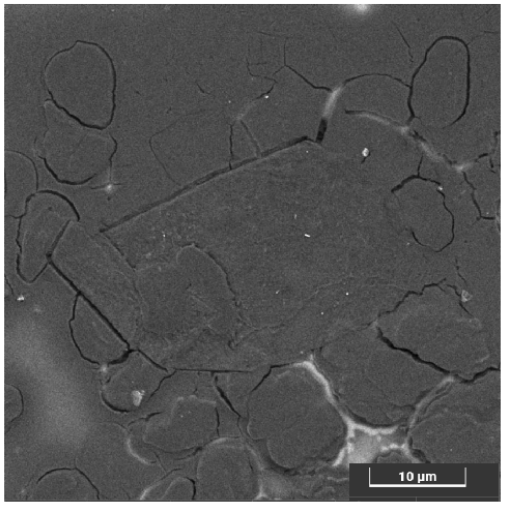

14

This third structure found in sample 1 shows two bodies having very well defined geometric lines with equally defined angles. The dimensions of these structures are a few tens of microns. In this case, we also report the photos in BSE as they are useful for visualizing the boundaries of the structure. The SE images show very bright edges (characteristic of this type of signal) to indicate that they are bodies with greater topographical relief. Looking at both images it is clear how these two structures detach from the support slide showing the regular edges very well. Furthermore, their texture looks very different from the rest of the sample. The images at higher magnifications, present in the following images, will highlight this aspect.

Ulteriori dettagli della texture ad ingrandimento crescenti.

More details of the texture at increasing magnification

SE

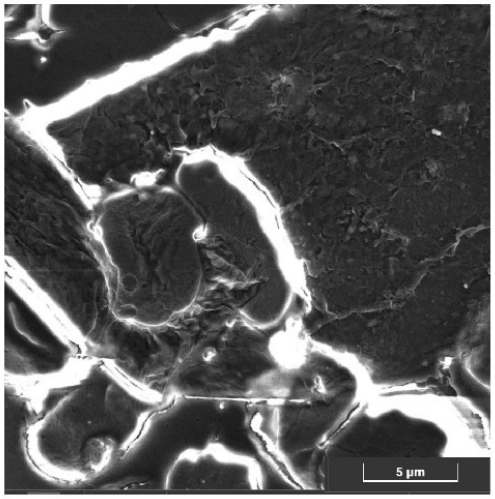

BSE

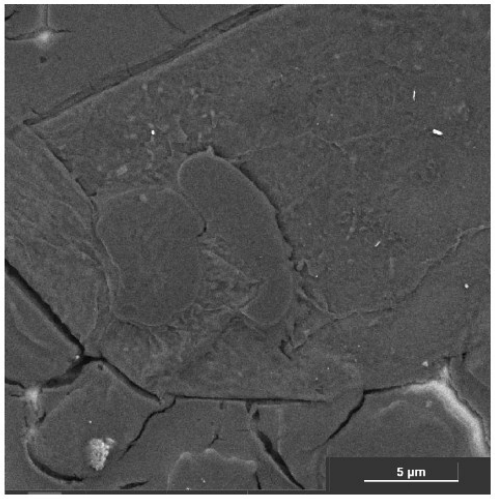

15

Il dettaglio ingrandito di uno di questi corpi mostra una struttura a film rugoso simile alle strutture di tipo grafenico.

SE

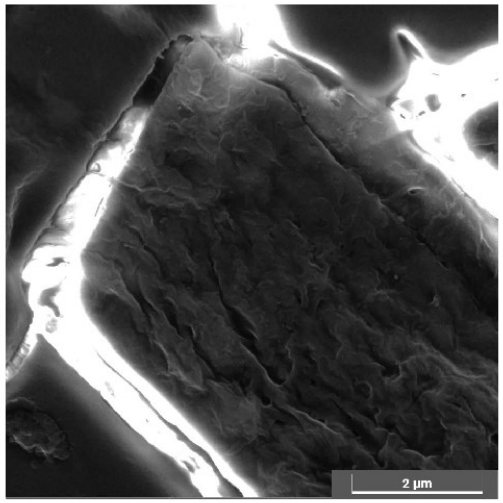

BSE

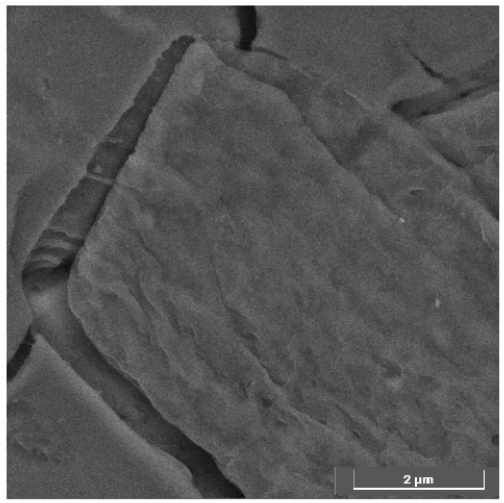

16

The enlarged detail of one of these bodies shows a wrinkled film structure like presumably graphenic particles.

In questa pagina vengono riportate le immagini acquisite a 6kx di un'ulteriore struttura rilevata nel campione 1.
In questo caso è molto utile riportare anche l'immagine in BSE che rende evidente già da subito il fatto che la composizione chimica di questo film è fatta di elementi molto leggeri (contrasto scuro rispetto al fondo) . Inoltre, si osserva come il film sia molto sottile in alcuni punti e le pieghe presenti siano molto ben visibili. Il film avvolge alcuni globuli rossi.
Le dimensioni sono di alcune decine di nanometri.

SE

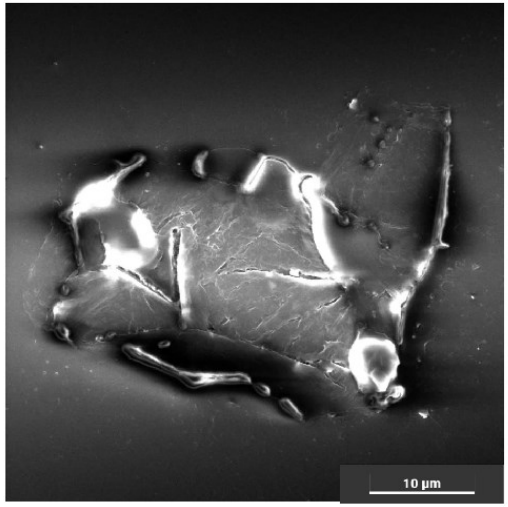

BSE

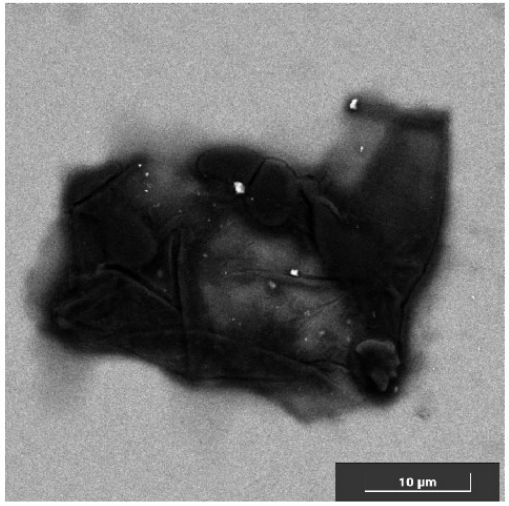

17

This page shows the images acquired at 6 kx of an additional structure detected in sample 1. In this case it is very useful to also report the image in BSE which makes it immediately evident that the chemical composition of this film is made of very light elements (dark contrast to the background). Furthermore, it is observed that the film is very thin in some points and the folds present are very clearly visible. The film surrounds some red blood cells. The dimensions are a few tens of nanometers.

Struttura 4_Dettaglio a 12kx C1

Due ingrandimenti in zone diverse, ad un ingrandimento maggiore 12kx, mostrano più in dettaglio la struttura del film.
Non appare continuo ma composto da più frammenti assemblati.

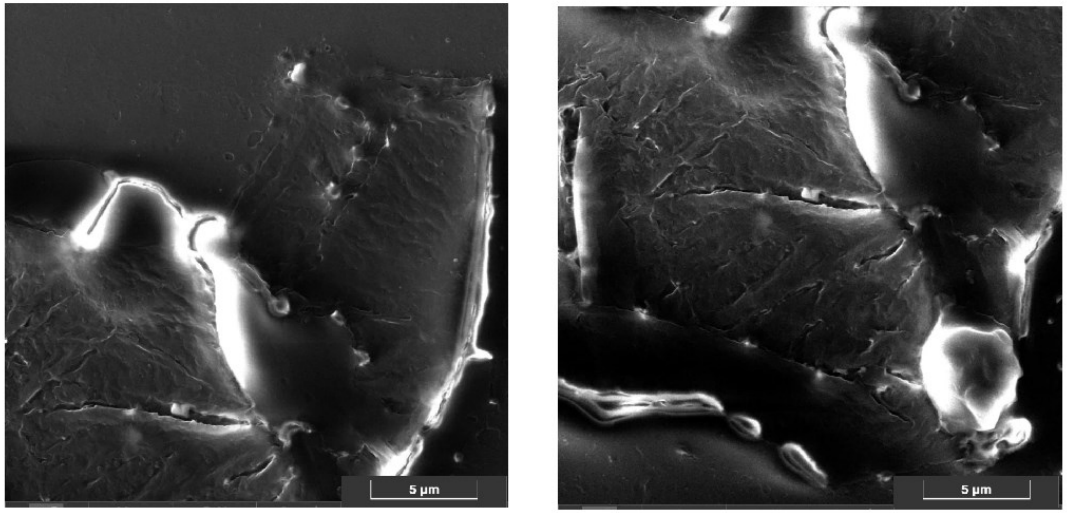

18

Two magnifications in different areas, at a magnification greater than 12 kx, show the structure of the film in more detail. It does not appear continuous but composed of several assembled fragments.

La mappa di distribuzione degli elementi conferma la prevalente presenza di carbonio con percentuali minori di azoto ed ossigeno.

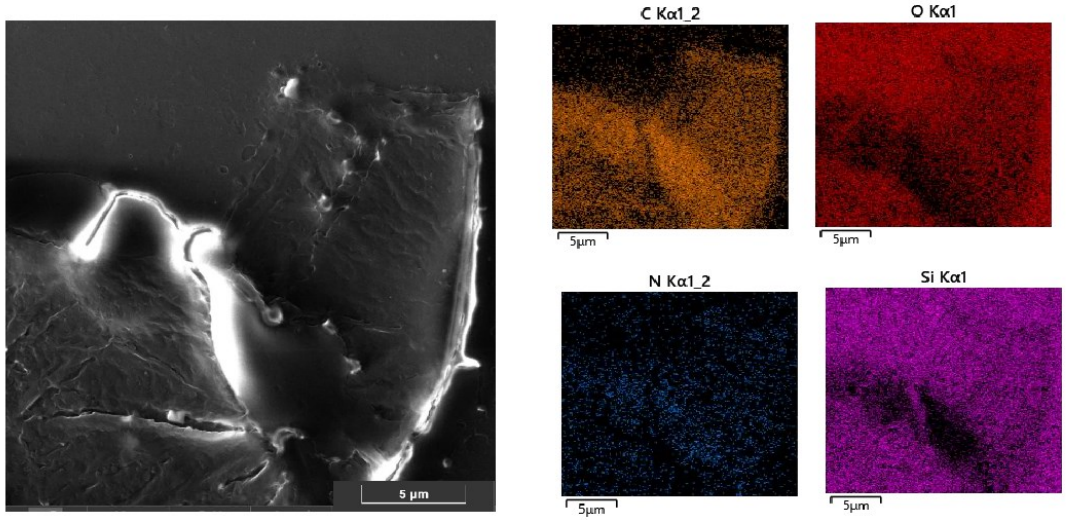

19

The distribution map of the elements confirms the prevalent presence of carbon with lower percentages of nitrogen and oxygen.

Qui riporto i dati della microanalisi eseguita in due punti: uno che sembra più spesso ed uno più sottile.
Nella parte ripiegata, e quindi più spessa (spettro 9) la presenza di silicio del vetrino è minore rispetto allo spettro 8 dove, essendo il film molto più sottile, la percentuale di silicio rilevata è molto maggiore.
Questo conferma quanto già detto nel caso della struttura 1 in pag.5.

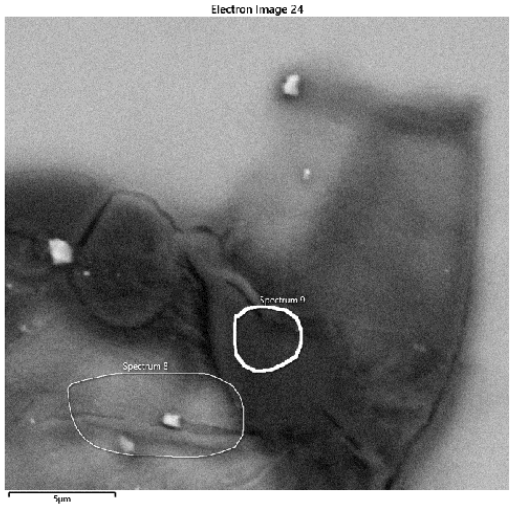

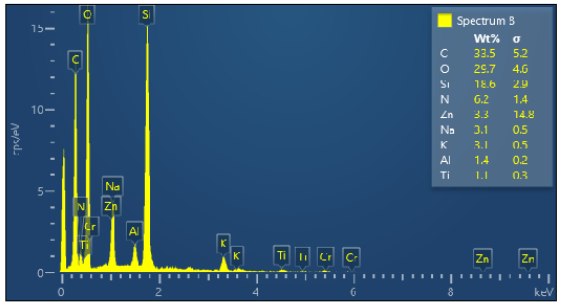

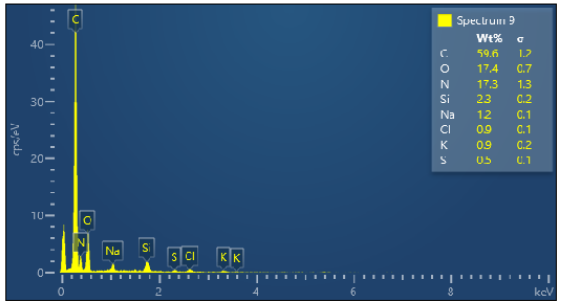

20

I report the data of the micro analysis performed in two points; one that looks thicker and one thinner. In the folded and therefore thicker part (spectrum 9) the presence of silicon in the slide is less than in spectrum 8, since the film is much thinner, the percentage of silicon is greater. This confirms what has already been said in the case of structure 1 on p. 5.

GLOBULI ROSSI_campione 2 C2

Immagine dei globuli rossi presenti nel campione 2.
I relativi dati della microanalisi mostrano la presenza di tracce di ferro uniformemente distribuiti.

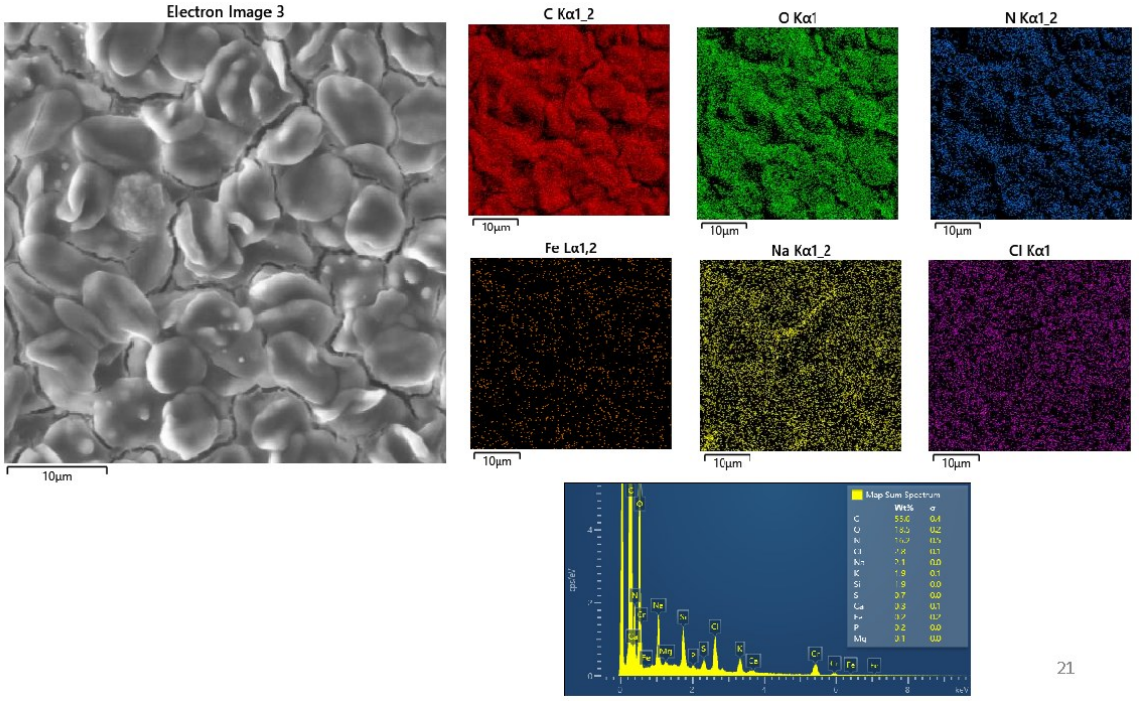

21

Image of the red blood cells presents, in the sample 2, the relative data of the micro analysis and shows the presence of traces of iron uniformly distributed.

Struttura 5_ 5kx C2

La prima struttura riscontrata nel secondo campione analizzato mostra un film di dimensioni notevoli (centinaia di micron) che avvolge i globuli rossi che appaiono molto agglomerati tra di loro.
In questo caso, ho ritenuto utile riportare anche l'immagine in BSE per evidenziare come il film avvolge i globuli in modo da non renderli più rilevabili.

SE

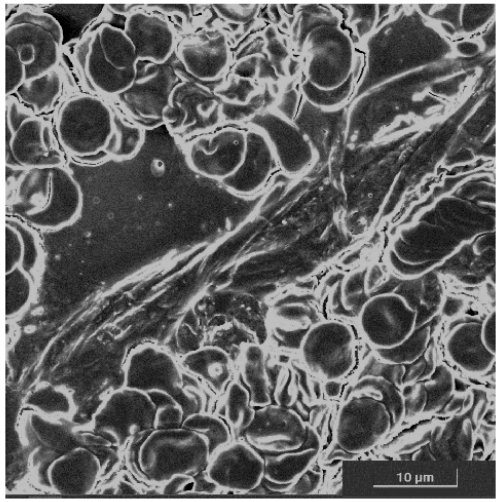

BSE

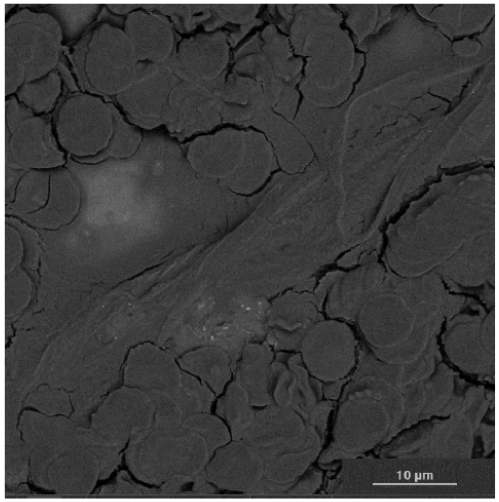

22

The first structure, found in the second sample analyzed, shows a film of considerable size (hundreds of microns) that surrounds the red blood cells which appears to be very agglomerated with each other. In this case, we found it useful to also bring the image back to BSE to highlight how the film wraps the blood cells so that they are no longer detectable.

La microanalisi eseguita in un punto del film, evidenzia una componente di prevalenza carboniosa. Inoltre sono anche state rilevate la presenza di ossigeno ed azoto in percentuali minori. .

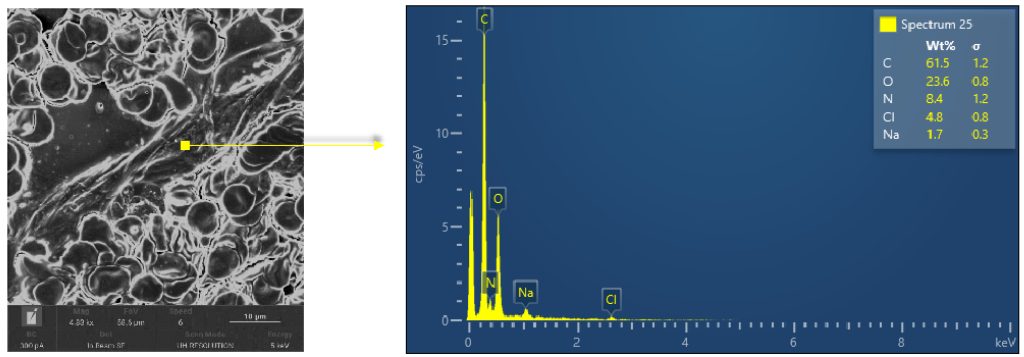

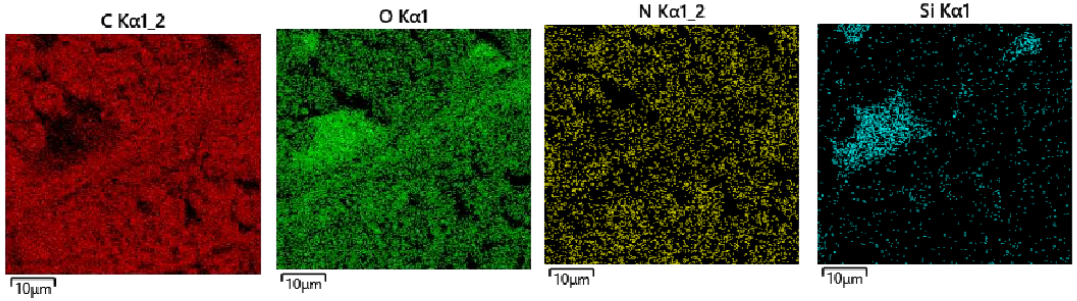

23

The micro analysis performed in one point of the film highlights a predominantly carbon component. In addition, the presence of oxygen and nitrogen in smaller percentages was also detected.

Quest'immagine mostra un altro frammento del film che, come una specie di velo, si estende per circa un centinaio di micron. Essendo così lungo, non è stato possibile fotografarlo in un solo scatto.

SE

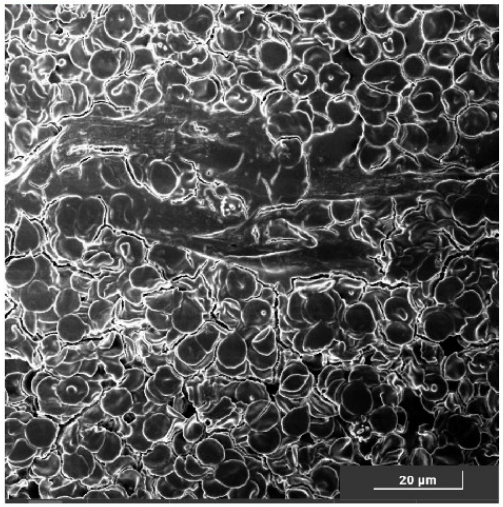

BSE

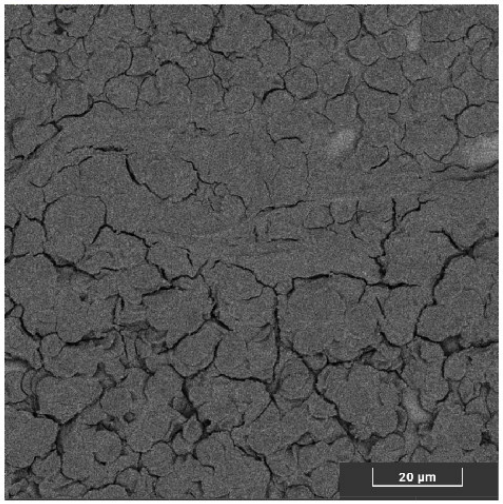

24

This image shows another fragment of the film which, like a veil, extends for about a hundred microns. Being so long, it wasn't possible to photograph it in one shot.

Struttura 5_Dettaglio ingrandito a 10kx C2

Dettaglio ingrandito del film con le sue pieghe dove si conferma la diversa natura del film rispetto ai globuli

SE

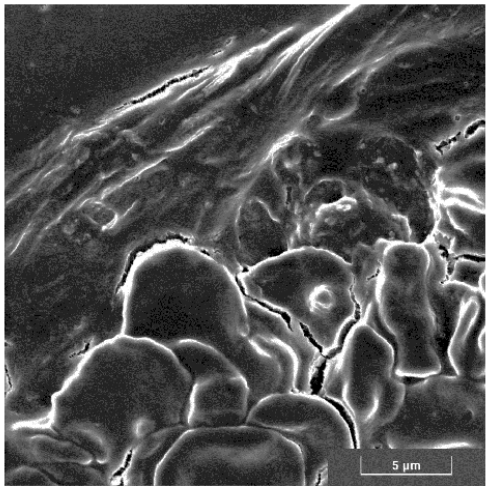

BSE

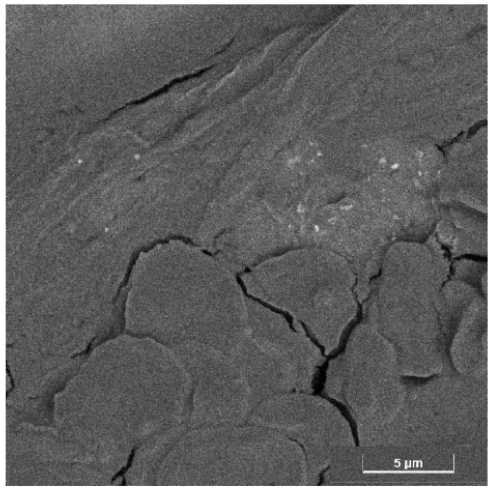

25

Enlarged detail of the film with its folds where the different nature of the film with respect to the globules is confirmed.

Struttura 5 a basso ingrandimento e misure C2

Su un'immagine a basso ingrandimento (circa 1kx) si è cercato di misurare la lunghezza del film utilizzando il software dello strumento. Come si osserva, la misura è approssimativa (in difetto) in quanto il film non è steso ma un po' ripiegato ed inoltre si tratta di più frammenti collegati. La misura complessiva supera i 200 micron

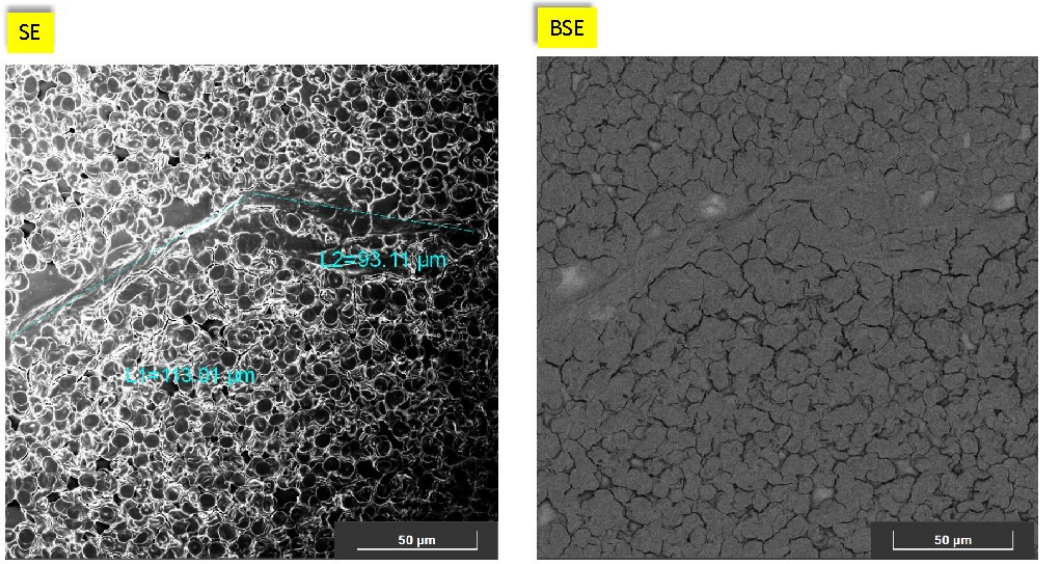

26

On a low magnification image (about 1 kx) an attempt was made to measure the length using the instrument software. As you can see, the measure is approximate (in default) as the film is not stretched but a little folded and moreover it is more connected fragments. The overall measurement exceeds 200 microns.

Struttura 6 C2

La seconda struttura riscontrata sul campione 2 mostra un film di circa 30 micron che avvolge dei globuli rossi.
Come si evidenzia da entrambe le immagini, il film appare molto sottile e formato da diversi frammenti assemblati e ripiegati.

SE

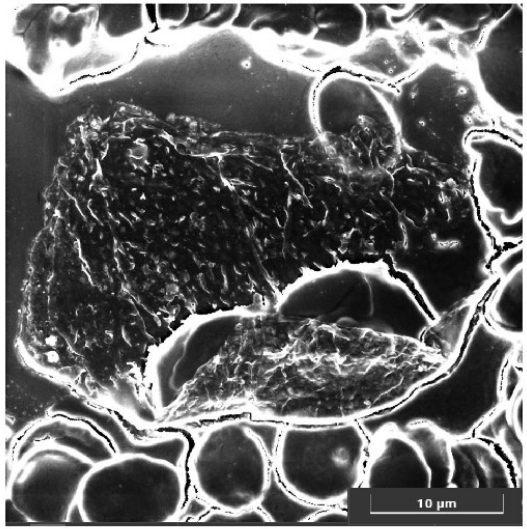

BSE

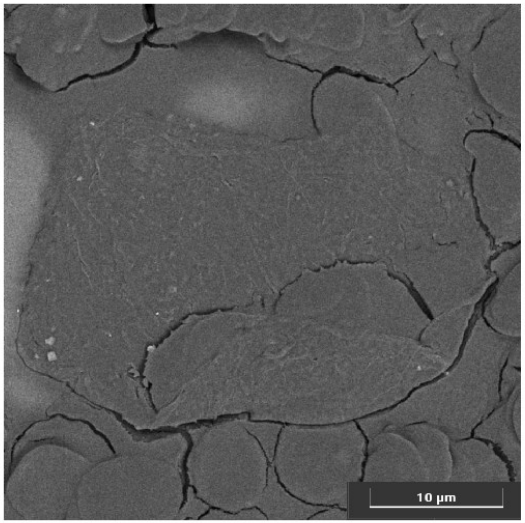

27

The second structure detected on sample 2 shows a film of about 30 microns that surrounds red blood cells. As evidenced by both images, the film appears very thin and made up of several assembled and folded fragments

L'immagine centrale mostra un dettaglio ingrandito a 36kx dell'area del riquadro del film.
Si osserva come il film appare composto da diversi strati assemblati. Non si tratta di un film continuo.
La microanalisi dell'area ingrandita conferma ancora una volta la presenza di carbonio, ossigeno ed azoto come componenti principali. Il fatto che il silicio del vetrino sia stato rilevato (al voltaggio utilizzato 5keV) ci dà informazioni sul fatto che il film è molto sottile.

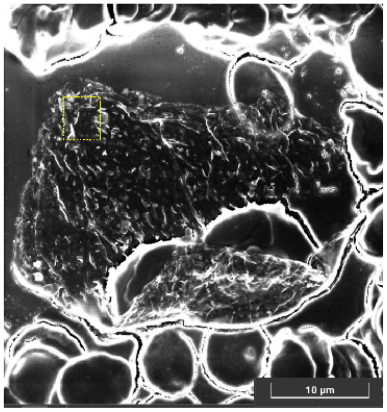

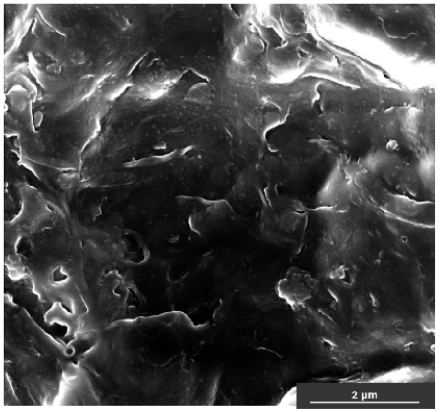

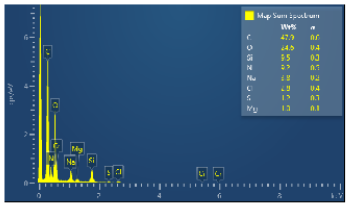

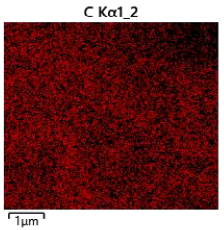

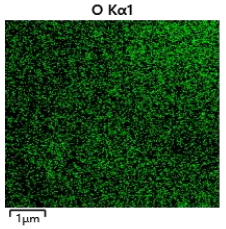

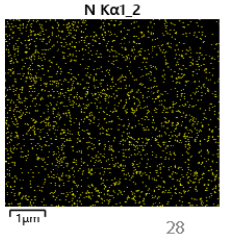

28

The central image shows an enlarged 30 kx detail of the film frame area. It is observed how the film appears to be composed of several assembled layers. This is not a continuous film. The micro analysis of the enlarged area once again confirms the presence of carbon, oxygen and nitrogen as main components. The fact that the silicon of the slide has been detected (at the voltage used 5kev) gives us information that the film is very thin

In queste pagine sono riportate le immagini relative ad un globulo rosso nel quale sono incastrati due tipi di agglomerati diversi:

1°agglomerati_freccia gialla: mostra strutture globulari formati da nanoparticelle che, visto il diverso livello di luminosità nell'immagine BSE, avranno composizione chimica diversa da quella dei globuli.

2°agglomerato_freccia rossa: Mostra una specie di melma che ingloba delle nanoparticelle incastrate nel globulo. In questo caso il livello di contrasto dell'immagine BSE ci suggerisce che la composizione chimica non sarà molto diversa da quella dei globuli

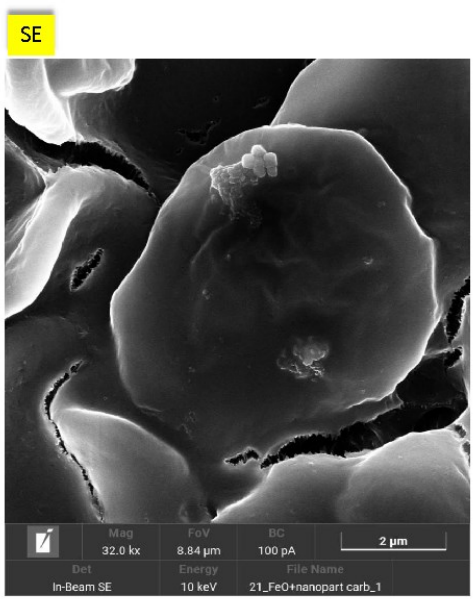

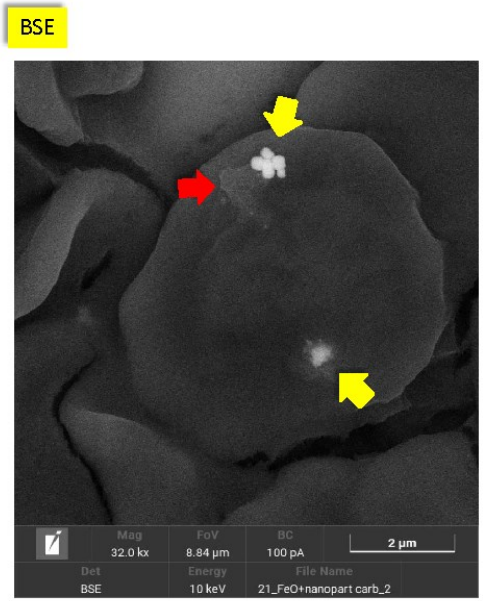

29

These pages show the images of a red blood cell in which two types of different agglomerates are stuck:

1st aggolmerate-yellow arrow: shows globular structures formed by nano particles which, given the different level of brightness in the BSE image, will have a chemical composition different from that of red blood cells.

2nd agglomerate-red arrow: shows a kind of slime that incorporates nano particles stuck in the globule. In this acso the contrast level of the BSE image suggests that the composition will not be very different from that of the blood cells.

Dettaglio ingrandito a 175kx degli agglomerati della parte superiore.
Le dimensioni degli agglomerati a destra sono di circa 200 nm e sono chiaramente composti da particelle di livello nanometrico (25-30 nm)

SE

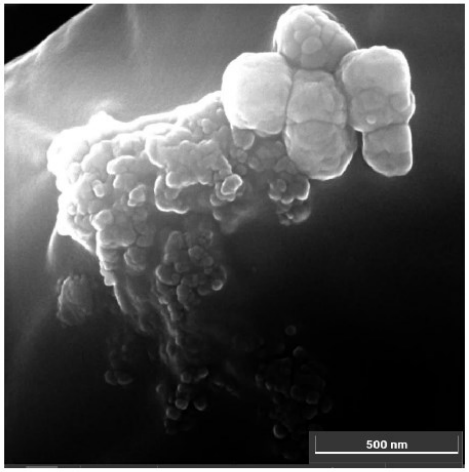

BSE

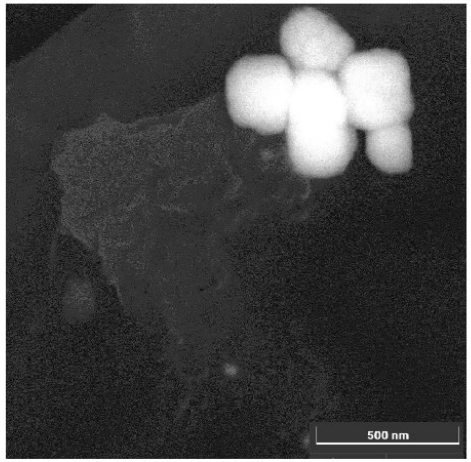

30

Detail enlarged to 175 kx of the agglomerations of the upper part.

The dimensions of the agglomerates on the right are about 200nm and are clarifications composed of particles at the nanometer level (25-30 nm).

Gli agglomerati di nanoparticelle della parte superiore (freccia gialla) sono agglomerati di ossido di ferro. Le mappe del ferro e dell'ossigeno mostrano degli accumuli in corrispondenza dell'agglomerato quindi, l'identificazione è certa.
Diversa è la situazione per l'agglomerato a fianco (freccia rossa) che, come si evince dalle mappe, sembra avere composizione carboniosa.

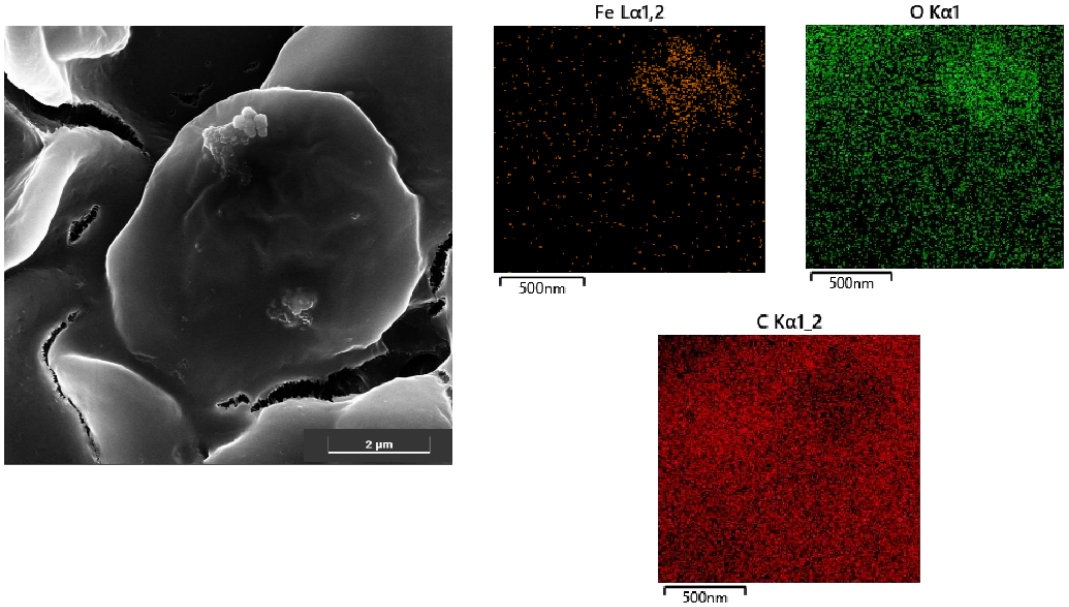

31

The agglomerates of nanoparticles in the upper part (yellow arrow) are agglomerates of iron oxide. The iron and oxygen maps show accumulations in correspondence with the agglomeration so the identification is certain. The situation of the adjacent agglomeration is different, which, as can be seen from the maps, seems to have a carbonaceous composition.

Osservando più da vicino l'agglomerato in basso, si evidenzia un blocco di dimensioni di qualche centinaia di nanometri dall'aspetto compatto avente composizione elementare analoga all'agglomerato riportato in pagina precedente: ferro ed ossigeno.
Le mappe di distribuzione degli elementi ci consentono di dire che si tratta, anche in questo caso, di ossido di ferro .

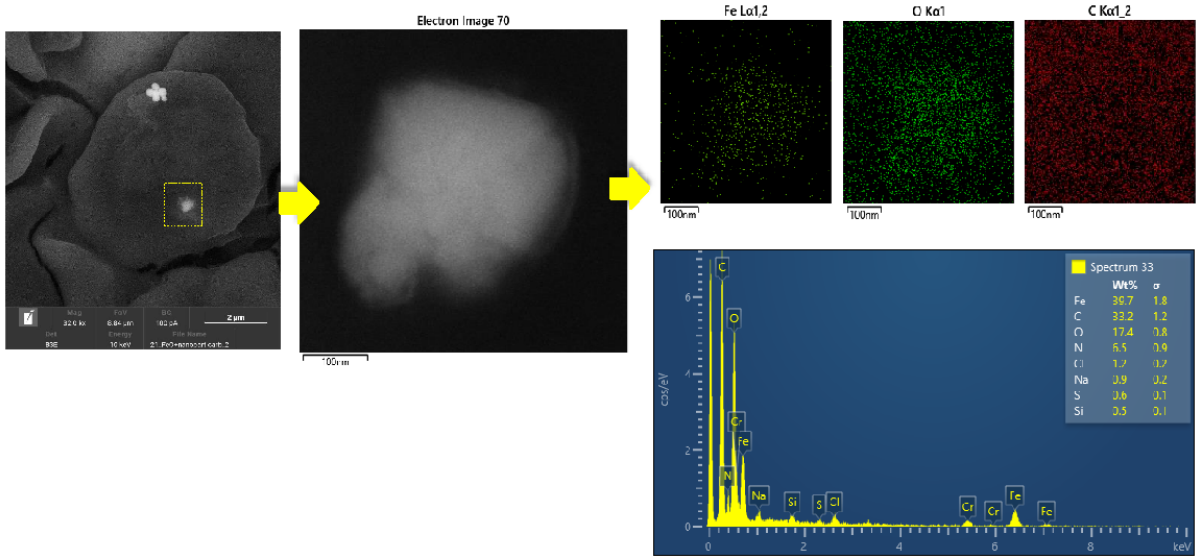

32

Observing the agglomerate at the bottom, a block of a few hundred nanometers dimensions is highlighted, with an elemental composition similar to the agglomerate shown on the previous page: iron and oxygen. The distribution maps of the elements allow us to say that it is iron oxide.

COMMENTI FINALI

In seguito a vostra richiesta, sono state condotte le misure con la tecnica FE-SEM/EDS su due campioni di sangue.
Gli strisci su vetrino sono stati preparati prima dell'esecuzione delle analisi e, appena asciutti, sono stati metallizzati con 1 nm di cromo.

Ogni campione analizzato è stato osservato in modo random fino al ritrovamento di strutture aventi morfologie «insolite» rispetto a quelle attese nel sangue umano. Durante la fase di identificazione, la scrivente è stata guidata dal committente nella scelta delle strutture dall'aspetto interessante che richiedevano un approfondimento e caratterizzazione.

Sono state riscontrate diverse «strutture» e, per ognuna di queste, si è proceduto acquisendo immagini a diversi ingrandimenti ed utilizzando i tre detector di cui è corredato il nostro strumento:
- Detector per elettroni secondari (SE)
- Detector per elettroni retrodiffusi (BSE)
- Detector per raggi X (EDS)

Le caratteristiche dei singoli segnali sono state descritte nella relazione tecnica a cui è allegato il presente report fotografico.

Sono state riscontrate strutture molto simili tra i due campioni, tranne per la struttura 7 (agglomerati di ossido di ferro) che è stata riscontrata solo per il campione 2.

La morfologia delle «strutture» maggiormente riscontrate può essere assimilabile a strutture di tipo grafenico: film sottili ripiegati e/o stropicciati simili ad un velo. I film appaiono sovrapposti ed agglomerati, talvolta sembrano assemblati gli uni agli altri ed in altri casi attorcigliati su se stessi. Le dimensioni riscontrate sono dell'ordine delle decine-centinaia di micron ma, essendo questi film visibilmente ripiegati, si tratta di misure approssimative (per difetto).

Per quanto riguarda la composizione chimica delle «strutture» riscontrate, queste hanno evidenziato una componente carboniosa prevalente accompagnata da percentuali ben più basse di ossigeno ed azoto tranne per la struttura 7 che, come citato sopra, era di natura completamente diversa: ferro ed ossigeno.

Un aspetto importante da sottolineare è che quando si ha a che fare con campioni composti da elementi leggeri presenti in una matrice avente composizione simile, come in questo caso, l' analisi elementare rappresenta una fase molto delicata dell'indagine.
Durante questo lavoro, infatti, sono state raccolte il maggior numero di informazioni possibili, sfruttando tutti i mezzi a disposizione, per consentire al committente di poter comprendere al meglio i campioni in questione.

Following your request, measurements were carried out with the FE-SEM / EDS technique on two blood samples.

The drops on the slide were prepared before carrying out the analyzes, and as soon as they were dry, they were metallized with 1 nm of chromium.

Each analyzed sample was observed randomly until structures with "unusual" morphologies compared to those expected in human blood were found. During the identification phase, the writer was guided by the client in the choice of structures with an interesting aspect that required in-depth analysis and characterization.

Different structures were found and for each of these we proceeded by acquiring images at different magnifications and using the three detectors that our instrument is equipped with:

- Secondary electron detector (SE)

- Detector for retro scattered electrons (BSE)

- X-ray detector (EDS)

The characteristics of the individual signals have been described in the technical report to which this photographic report is attached.

Very similar structures were found between the two samples except for figure 7 (iron oxide agglomerates) which was found only for sample 2.

The morphology for the most commonly encountered structures can be assimilated to structures presumably graphenic folded and / or wrinkled thin films similar to a veil. The films appear superimposed and agglomerated, sometimes they seem assembled to each other and in other cases twisted on themselves. The dimensions found are of the order of tens-hundreds of microns but, as these films are visibly folded, these are approximate measures (by default).

As regards the chemical composition of the structures found, these showed a prevalent carbon component accompanied by much lower percentages of oxygen and nitrogen except for structure 7 which, as mentioned above, was of a completely different nature: iron and oxygen.

An important aspect to underline is that when dealing with samples composed of light elements present in a matrix having a similar composition, as in this case, the elemental analysis becomes a very delicate phase of the investigation.

During this work, in fact, as much information as possible was collected, exploiting all the means available, to allow the client to better understand the samples in question.

Legal Disclaimer

The information on the website and in the ***IJVTPR*** is not intended as a diagnosis, recommended treatment, prevention, or cure for any human condition or medical procedure that may be referred to in any way. Users and readers who may be parents, guardians, caregivers, clinicians, or relatives of persons impacted by any of the morbid conditions, procedures, or protocols that may be referred to, must use their own judgment concerning specific applications. The contributing authors, editors, and persons associated in any capacity with the website and/or with the journal disclaim any liability or responsibility to any person or entity for any harm, financial loss, physical injury, or other penalty that may stem from any use or application in any context of information, conclusions, research findings, opinions, errors, or any statements found on the website or in the ***IJVTPR***. The material presented is freely offered to all users who may take an interest in examining it, but how they may choose to apply any part of it, is the sole responsibility of the viewer/user. If material is quoted or reprinted, users are asked to give credit to the source/author and to conform to the non-commercial, no derivatives, requirements of the Creative Commons License 4.0 NC ND